Research Paper

PAIN®

Interleukin-6-mediated functional upregulation of TRPV1 receptors in dorsal root ganglion neurons through the activation of JAK/PI3K signaling pathway: roles in the development of bone cancer pain in a rat model

Dong Fang[a,b], Ling-Yu Kong[a,b], Jie Cai[a,b], Song Li[a,b], Xiao-Dan Liu[a,b], Ji-Sheng Han[a,b,c], Guo-Gang Xing[a,b,c,*]

Abstract

Primary and metastatic cancers that affect bone are frequently associated with severe and intractable pain. The mechanisms underlying the pathogenesis of bone cancer pain still remain largely unknown. Previously, we have reported that sensitization of primary sensory dorsal root ganglion (DRG) neurons contributes to the pathogenesis of bone cancer pain in rats. In addition, numerous preclinical and clinical studies have revealed the pathological roles of interleukin-6 (IL-6) in inflammatory and neuropathic hyperalgesia. In this study, we investigated the role and the underlying mechanisms of IL-6 in the development of bone cancer pain using in vitro and in vivo approaches. We first demonstrated that elevated IL-6 in DRG neurons plays a vital role in the development of nociceptor sensitization and bone cancer–induced pain in a rat model through IL-6/soluble IL-6 receptor (sIL-6R) trans-signaling. Moreover, we revealed that functional upregulation of transient receptor potential vanilloid channel type 1 (TRPV1) in DRG neurons through the activation of Janus kinase (JAK)/phosphatidylinositol 3-kinase (PI3K) signaling pathway contributes to the effects of IL-6 on the pathogenesis of bone cancer pain. Therefore, suppression of functional upregulation of TRPV1 in DRG neurons by the inhibition of JAK/PI3K pathway, either before surgery or after surgery, reduces the hyperexcitability of DRG neurons and pain hyperalgesia in bone cancer rats. We here disclose a novel intracellular pathway, the IL-6/JAK/PI3K/TRPV1 signaling cascade, which may underlie the development of peripheral sensitization and bone cancer–induced pain.

Keywords: Bone cancer pain, Dorsal root ganglion, Interleukin-6, TRPV1, Janus kinase, Phosphatidylinositol 3-kinase, Hyperexcitability

1. Introduction

Bone cancer pain has a strong impact on the quality of life of patients but is difficult to treat. The mechanisms underlying the development of bone cancer–induced pain are largely unknown. We have previously suggested that the sensitization of primary sensory dorsal root ganglion (DRG) neurons contributes to the pathogenesis of bone cancer pain in rats.[81] Inflammatory mediators released from damaged nerves and/or the tumor site are implicated in the sensitization of primary sensory neurons.[46,61]

Interleukin-6 (IL-6) is a proinflammatory cytokine known to be involved in several inflammatory and neuropathic hyperalgesia.[47,59,66,72] An increase of IL-6 mRNA levels in the spinal cord is found in a rat model of bone cancer pain.[19] However, whether IL-6 contributes to the sensitization of DRG neurons and the development of bone cancer pain still remains unclear.

Interleukin-6 exerts its biological effect on target cells either through classic signaling by binding to membrane-bound receptor mIL-6R or through trans-signaling by binding to soluble receptor sIL-6R.[65] The binding of IL-6 to mIL-6R or sIL-6R induces homodimerization of glycoprotein 130 (gp130), a common signal transduction receptor subunit, resulting in activation of Janus kinase (JAK)/signal transducer and activator of transcription (STAT), mitogen-activated protein kinase (MAPK)/extracellular signal–regulated kinases (ERKs) and phosphatidylinositol 3-kinase (PI3K)/AKT signaling pathways.[20,21,52] The IL-6/gp130 complex has been shown to be involved in heat hypersensitivity by increasing transient receptor potential vanilloid channel type 1 (TRPV1) currents through the activation of Gab1/2/PI3K/Protein kinase C (PKC)-δ signaling pathway both in vitro and in vivo.[2,58] Upregulation of TRPV1 expression[24,57,60] and sensitization of TRPV1 channels[77] in DRG neurons are found to be associated with thermal hyperalgesia after cancer infiltration in rodents. Selective blockade of TRPV1 results in a significant attenuation of nociceptive behaviors in bone cancer pain models.[23,35,56] These findings support a role for TRPV1 in the pathogenesis of bone cancer pain.

Sponsorships or competing interests that may be relevant to content are disclosed at the end of this article.

[a] Neuroscience Research Institute, Peking University, Beijing, China, [b] Department of Neurobiology, School of Basic Medical Sciences, Peking University, Beijing, China, [c] Key Laboratory for Neuroscience, Ministry of Education/National Health and Family Planning Commission, Beijing, China

**Corresponding author. Address: Neuroscience Research Institute and Department of Neurobiology, Peking University, 38 Xue-Yuan Rd, Hai-Dian District, Beijing 100191, China. Tel.: +8610-8280-1067; fax: +8610-8280-1067. E-mail address: ggxing@bjmu.edu.cn.*

Supplemental digital content is available for this article. Direct URL citations appear in the printed text and are provided in the HTML and PDF versions of this article on the journal's Web site (www.painjournalonline.com).

PAIN 156 (2015) 1124–1144

http://dx.doi.org/10.1097/j.pain.0000000000000158

Several lines of evidence have shown that PI3K regulates the activity of TRPV1 by working at the levels of transcription, translation, and posttranslation.[34,50,80] Activation of JAK seems to play a major role in IL-6-mediated thermal hyperalgesia and sensitization of heat-activated TRPV1 channels.[58] It raises the possibility that the JAK/PI3K signaling pathway is likely involved in IL-6-mediated upregulation and sensitization of TRPV1 channels.

In this study, we investigated the role and the underlying mechanism of IL-6 in the development of bone cancer pain using in vitro and in vivo approaches. We provide valid evidence showing that enhanced IL-6 plays a crucial role in the sensitization of DRG neurons and the development of bone cancer pain in a rat model through IL-6/sIL-6R trans-signaling. Moreover, we suggest that functional upregulation of TRPV1 in DRG neurons through the activation of JAK/PI3K signaling pathway underlies the effects of IL-6 on the pathogenesis of bone cancer pain.

2. Materials and methods

2.1. Chemicals, antibodies, and animals

IL-6, sIL-6R and sgp130 were purchased from R&D Systems (Minneapolis, MN) and were dissolved in sterile 0.01 M phosphate-buffered saline (PBS) as a 100 μg/mL stock solution, stored at −20°C, and diluted to desired concentrations just before the experiments. AG490 (JAK inhibitor), PD98059 (MEK [ERK kinase] inhibitor), and LY294002 (PI3K inhibitor) were purchased from Cell Signaling Technology (Beverly, MA) and were dissolved in sterile 5% dimethyl sulfoxide (DMSO) with 95% saline solution. Anisomycin (a general protein synthesis inhibitor) was obtained from Merck-Calbiochem (Darmstadt, Germany) and was dissolved in 5% DMSO. Capsaicin (TRPV1 agonist), capsazepine (TRPV1 inhibitor), trypsin, collagenase IA, and poly-D-lysine were purchased from Sigma-Aldrich (Saint Louis, MO). Neurobasal growth medium and B27 supplement were purchased from Life Technologies (Carlsbad, CA). Sulfo-NHS-LC-Biotin was obtained from Pierce (Rockford, IL).

Polyclonal rabbit anti-rat IL-6 antibody was obtained from Sigma-Aldrich. Polyclonal rabbit anti-rat IL-6R, rabbit anti-rat gp130, and rabbit anti-rat TRPV1 antibodies were obtained from Santa Cruz Biotechnology (Santa Cruz, CA). Polyclonal rabbit anti–phosphorylated-AKT (Ser473) and rabbit anti-AKT antibodies were purchased from Cell Signaling Technology. Monoclonal mouse anti-rat transferrin receptor (TfR) antibody was obtained from Life Technologies. Monoclonal mouse anti-rat β-actin antibody and horseradish peroxidase–conjugated secondary antibodies including goat anti-rabbit IgG and goat anti-mouse IgG were purchased from Santa Cruz Biotechnology. All other chemicals or reagents were obtained from Sigma, Invitrogen, or Pierce except as mentioned in the text.

Female Sprague–Dawley rats weighing 150 to 180 g at the beginning of the experiments were provided by the Department of Experimental Animal Sciences, Perking University Health Science Center. The rats were housed in separate cages with free access to food and water. The room temperature was kept at 24°C ± 1°C under a natural light–dark cycle. All animal experimental procedures were conducted in accordance with the guidelines of the International Association for the Study of Pain[84] and were approved by the Animal Care and Use Committee of Peking University.

2.2. Inoculation of tumor cells

Mammary rat metastasis tumor (MRMT-1) cells (carcinoma) were kindly provided by Novartis Oncology Research, Basel. A rat model of bone cancer pain was established by intratibial injection of syngeneic MRMT-1 rat mammary gland carcinoma cells as described in our previous studies.[44,82] Briefly, after anesthetized with 10% chloral hydrate (0.3 g/kg, intraperitoneally [i.p.]), the left tibia of rat was carefully exposed and a 23-gauge needle was inserted in the intramedullary canal of the bone. It was then removed and replaced with a long, thin blunt needle attached to a 10-μL Hamilton syringe containing the medium to be injected. A volume of 4 μL MRMT-1 rat mammary gland carcinoma cells (4×10^4) or vehicle (PBS) was injected into the tibial bone cavity. After injection, the site was sealed with bone wax and the wound was finally closed. None of the animals showed sign of motor dysfunction after inoculation of tumor cells.

2.3. Behavioral studies

All behavioral experiments were performed blinded to treatment group.

2.3.1. Assessment of mechanical allodynia

Mechanical allodynia, as a behavioral sign of bone cancer pain, was assessed by measuring 50% paw withdrawal threshold (PWT) as described in our previous reports.[16,29] The 50% PWT in response to a series of von Frey filament (Stoelting, Wood Dale, IL) was determined by the Up-and-Down method.[13] The rat was placed on a metal mesh floor covered with an inverted clear plastic cage and allowed a 20-minute period for habituation. Eight von Frey filaments with approximately equal logarithmic incremental (0.224) bending forces were chosen (0.41, 0.70, 1.20, 2.00, 3.63, 5.50, 8.50, and 15.10*g*). Each trial started with a von Frey force of 2*g* delivered perpendicularly to the plantar surface of the left hind paw for about 2 to 3 seconds. An abrupt withdrawal of the foot during stimulation or immediately after the removal of the filament was recorded as a positive response. Whenever there was a positive or negative response, the next weaker or stronger filament was applied, respectively. This procedure was performed until 6 stimuli after the first change in response had been observed. The 50% PWT was calculated using the following formula: $50\%\ \mathrm{PWT} = 10^{[X_f + k\delta]}$, where X_f is the value of the final von Frey filament used (in log units), k is a value measured from the pattern of positive/negative response, and $\delta = 0.224$, which is the average interval (in log units) between the von Frey filaments.[17] If an animal responded to the lowest von Frey filament, a value of 0.25*g* was assigned. If an animal did not respond to the highest von Frey filament, the value was recorded as 15.0*g*. In rats, mechanical allodynia is assessed by measuring the 50% PWT to von Frey filaments, and an allodynic rat is defined as that the 50% PWT is $<4.0g$ (ie, withdrawal in response to non-noxious tactile stimulus).[85]

2.3.2. Assessment of thermal hyperalgesia

Thermal hyperalgesia of the hind paws was tested as described by our previous studies.[44,45] Rats were allowed to acclimate for a minimum of 30 minutes within acrylic enclosures on a clear glass plate maintained at 30°C. A radiant heat source was focused onto the plantar surface of the hind paw. Measurement of paw withdrawal latency (PWL) was taken by a timer that was started by the activation of the heat source and stopped when withdrawal of the paw was detected with a photodetector. A maximal cutoff time of 30 seconds was used to prevent unnecessary tissue damage. Three measurements of PWL were taken for ipsilateral hind paw and were averaged as the result of

each test session. The hind paw was tested with greater than 5-minute intervals between consecutive tests.

2.3.3. Implantation of intrathecal catheter

Under chloral hydrate (0.3 g/kg, i.p.) anesthesia, implantation of an intrathecal cannula was performed following our previous methods.[22,63] Briefly, a PE-10 polyethylene catheter was implanted between the L5 and L6 vertebrae to reach the lumbar enlargement of the spinal cord. The outer part of the catheter was plugged and fixed onto the skin on closure of the wound. All surgical procedures were performed under sterile conditions. Rats showing neurological deficits after the catheter implantation were euthanized. Drugs or vehicles were intrathecally injected through the implanted catheter in a 10-μL volume of solution followed by 10 μL of vehicle for flushing. Each injection lasted at least 5 minutes. After an injection, the needle remained in situ for 2 minutes before being withdrawn.

2.3.4. Measurement of drug effects on pain behaviors

The first behavioral experiment was performed to examine whether FIL-6, a fused IL-6/sIL-6R complex (ie, a mixture of IL-6 together with sIL-6R) could mimic pain hypersensitivity in normal rats. Effects of intrathecal administration of FIL-6 (100 ng in a 10-μL volume) on ipsilateral PWT responding to von Frey filaments and PWL to radiant heat stimuli were measured just before drug injection and then were measured at 0.5, 1, 12, 24, and 48 hours after drug injection, respectively. We used a higher dose of FIL-6 (100 ng in a 10-μL volume) for the purpose of observing the long-lasting effects (48 hours) of IL-6 on pain behaviors as described in previous studies.[7,66,73] It has been shown that a lower dose of IL-6 (10 ng/mL) is also sufficient to induce heat hyperalgesia in rats[36]; however, its maximal action of 2 hours is not suitable for examining the long-term effects of IL-6. In fact, our preliminary data revealed that the longest effect of FIL-6 on pain behaviors is merely 2 hours after an intrathecal dose of 10 ng/mL and 6 hours after an intrathecal does of 50 ng/mL (supplementary data, Fig. S1, available online as Supplemental Digital Content at http://links.lww.com/PAIN/A62). To determine by which signaling pathway (classic signaling or trans-signaling) FIL-6 exerts its influence on pain behaviors, soluble gp130 (sgp130, 100 ng/10 μL), a potent IL-6/sIL-6R trans-signaling inhibitor, was intrathecally administrated to rats 30 minutes before FIL-6 application, and the same behavioral test was measured as described above.

The second behavioral experiment was conducted to explore whether IL-6 contributes to the development of bone cancer–induced pain through a trans-signaling pathway. Effects of pretreatment or posttreatment with sgp130 (a potent IL-6/sIL-6R trans-signaling inhibitor) on bone cancer–induced pain were examined in MRMT-1 rats, respectively. In the pretreatment experiments, sgp130 (100 ng/10 μL) was intrathecally administrated to MRMT-1 rats once per day from day 7 to day 13 after tumor cell inoculation, based on our previous findings that animals displayed no significant pain hypersensitivity at day 7 after tumor cell inoculation.[81] The ipsilateral PWT and PWL of animals were measured on day 14 after tumor cell inoculation. In the posttreatment experiments, sgp130 (100 ng/10 μL) was intrathecally administrated to MRMT-1 rats once per day from day 15 to day 17 after tumor cell inoculation, based on the previous reports that stable mechanical allodynia and thermal hyperalgesia were both seen at day 15 after tumor cell inoculation.[81] The ipsilateral PWT and PWL of rats were measured on the day before inoculation surgery (day 0) as the baseline and were then evaluated on the day before drug application (14 days after surgery, day 14) and on day 3 after drug injection (18 days after surgery, day 18), respectively.

To further clarify whether the activation of TRPV1 through JAK/PI3K signaling pathway was involved in FIL-6-mediated pain hypersensitivity, we also performed behavioral experiments to investigate the effects of AG490 (a JAK inhibitor), LY294002 (a PI3K inhibitor), and capsazepine (CPZ, a TRPV1 receptor inhibitor) on FIL-6-evoked mechanical allodynia and thermal hyperalgesia in normal rats, respectively. AG490 (10 nmol), LY294002 (10 nmol), or CPZ (20 μg) in a 10-μL volume was intrathecally administrated to rats 30 minutes before FIL-6 (100 ng/10 μL) application. The effects of each inhibitor on FIL-6-evoked mechanical allodynia and thermal hyperalgesia were measured just before FIL-6 injection and were then measured at 0.5, 1, 12, 24, and 48 hours after FIL-6 injection, respectively.

Next, we conducted behavioral experiments to determine whether inhibition of TRPV1 receptors in DRG neurons with CPZ would attenuate the bone cancer–induced pain hypersensitivity in MRMT-1 rats. CPZ (20 μg) in a 10-μL volume was intrathecally delivered to cancer rats twice per day from day 15 to day 17 after tumor cell inoculation. The ipsilateral PWT and PWL of rats were tested on the day before inoculation surgery (day 0, designated as the baseline) and were then evaluated on the day before drug application (14 days after surgery, day 14) and on days 3, 4, and 5 after the first drug injection (ie, 18, 19, and 20 days after surgery, days 18, 19, and 20), respectively.

Furthermore, we performed behavioral experiments to study whether the JAK/PI3K signaling pathway was associated with the development of bone cancer pain. Effects of pretreatment or posttreatment with the JAK/PI3K pathway inhibitor on bone cancer–induced pain were examined in MRMT-1 rats, respectively. In the pretreatment experiments, JAK inhibitor AG490 (10 nmol) or PI3K inhibitor LY294002 (10 nmol) in a 10-μL volume was intrathecally administrated to MRMT-1 rats once per day from day 7 to day 13 after tumor cell inoculation, based on our previous findings that animals displayed no significant pain hypersensitivity at day 7 after tumor cell inoculation.[81] The ipsilateral PWT and PWL of rats were measured on day 14 after tumor cell inoculation. In the posttreatment experiments, AG490 (10 nmol) or LY294002 (10 nmol) in a 10-μL volume was intrathecally administrated to MRMT-1 rats once per day from day 15 to day 17 after tumor cell inoculation, based on the previous reports that both stable mechanical allodynia and thermal hyperalgesia were seen at day 15 after tumor cell inoculation.[81] The ipsilateral PWT and PWL of rats were measured on the day before inoculation surgery (day 0) as the baseline and were then evaluated on the day before drug application (14 days after surgery, day 14) and on day 3 after drug injection (18 days after surgery, day 18), respectively.

In addition, to determine whether there is a role for these signaling pathways (IL-6/JAK/PI3K/TRPV1) at the peripheral terminals of DRG neurons in bone cancer–induced hyperalgesia, we performed 2 additional experiments that examined the effects of all inhibitors used for these signaling pathways (eg, sgp130 [an IL-6 trans-signaling pathway inhibitor], AG490 [a JAK inhibitor], LY294002 [a PI3K inhibitor], and capsazepine [CPZ, a TRPV1 receptor inhibitor]), on IL-6- and bone cancer–induced pain hypersensitivity by intraplantar injection of each inhibitor. In the first experiments, sgp130 (100 ng), AG490 (10 nmol), LY294002 (10 nmol), or CPZ (20 μg) in a 10-μL volume was intraplantarly delivered to normal rats 30 minutes before FIL-6 (100 ng/10 μL) application. The effects of each inhibitor on FIL-6-evoked

mechanical allodynia and thermal hyperalgesia were measured just before FIL-6 injection and were then measured at 1, 24, and 48 hours after FIL-6 injection, respectively (see supplementary data, Fig. S2 available online as Supplemental Digital Content at http://links.lww.com/PAIN/A63). In the second experiments, sgp130 (100 ng), AG490 (10 nmol), LY294002 (10 nmol), or CPZ (20 μg) in a 10-μL volume was intraplantarly delivered to cancer rats once per day from day 7 to day 13 after tumor cell inoculation, based on our previous findings that animals displayed no significant pain hypersensitivity at day 7 after tumor cell inoculation.[81] The ipsilateral PWT and PWL of the animals were measured on days 14, 16, and 18 after tumor cell inoculation (see supplementary data, Fig. S3 available online as Supplemental Digital Content at http://links.lww.com/PAIN/A64).

2.3.5. Assessment of locomotor function

The inclined plate test was used for the assessment of locomotor function. Each rat was placed crosswise to the long axis of an inclined plate. The initial angle of the inclined plate was 50°. The angle was then adjusted in 5° increments. The maximum angle of the plate on which the rat maintained its body position for 5 seconds without falling was determined according to the method reported by Rivlin and Tator.[64] In this study, inclined plate test was performed for all behavioral experiments in which the animals received intrathecal drugs.

2.4. Primary culture and acute dissociation of dorsal root ganglion neurons

Primary culture of DRG neurons was performed according to the modified method described by Natura et al.[53] In brief, rats (age, 2-3 weeks) were euthanized with ether and DRG were dissected from lumbar spinal segments. The DRG were digested with collagenase type IA (3 mg/mL, Sigma) for 45 minutes and 0.25% trypsin (Type II-S, Sigma-Aldrich) for another 12 minutes at 37°C. After terminating the enzymatic treatment by Dulbecco's modified Eagle medium plus 10% fetal bovine serum, ganglia were dissociated with a polished Pasteur pipette and the suspension of ganglia was sieved through a filter to remove debris and centrifugated at 800 rpm for 2 minutes. The resuspended cells were plated on 35-mm dishes coated with poly-D-lysine (0.5 mg/mL, Sigma-Aldrich), kept for 3 hours, and replaced with Neurobasal growth medium containing B27 supplement, 0.5 mM L-GlutaMAX (Sigma-Aldrich), 100 U/mL penicillin, and 100 mg/mL streptomycin. The cells were kept at 37°C in an incubator with 5% CO_2 and 95% air. Cultures were fed daily with Neurobasal growth medium containing B27 supplement. These primary cultured DRG neurons were prepared for the treatment of FIL-6 (cultured with FIL-6 or FIL-6 plus different inhibitors) to investigate short-term (10-90 minutes) and long-term (6-48 hours) effects of FIL-6 on functional TRPV1 expression.

Acute dissociation of DRG neurons was performed as described in our previous reports.[44,82] In brief, neurons were isolated from L4 and L5 DRG of adult rats and were digested using the same procedure as described for cell culturing above. The dissociated cells were placed on poly-D-lysine (0.5 mg/mL, Sigma)–treated glass coverslips contained within 4-well sterile tissue culture plates and kept in 5% CO_2 incubator at 37°C for 2 to 3 hours before patch-clamp recording or FIL-6 treatment. These acutely isolated DRG neurons obtained from adult normal rats and the bone cancer rats with different treatments were used for transient electrophysiological studies.

2.5. Western blot analysis

2.5.1. Total protein preparation

Under deep anesthesia with 10% chloral hydrate (0.3 g/kg, i.p.), the rat L4–L5 DRG and the liver tissue were removed and immediately homogenized in ice-chilled lysis buffer containing 50 mM Tris (pH 8.0), 150 mM NaCl, 1% NP40 (Sigma-Aldrich), 0.5% sodium deoxycholate (Sigma-Aldrich), 0.1% sodium dodecyl sulfate (SDS), and protease inhibitor cocktail (Roche, Indianapolis, IN). In some experiments, the cultured DRG neurons were also lysed with the same lysis buffer. Then, the homogenates were centrifuged at 12,000 rpm for 10 minutes at 4°C, and the supernatant was analyzed. The concentration of protein was measured with a BCA assay kit (Pierce), and an equal amount of protein samples was denatured and then analyzed by Western blot.

2.5.2. Membrane protein preparation

Preparation of membrane fraction was performed in DRG neurons as previously described.[71] In brief, L4 and L5 DRG were homogenized in a glass dounce in ice-chilled lysis buffer containing 0.3 M sucrose, 10 mM Tris (pH 8.1), 2 mM EDTA, 1 mM phenylmethanesulfonyl fluoride (PMSF), 1 mM dithiothreitol (DTT), and protease inhibitor cocktail (Roche). Homogenates were kept on ice for 1 hour before centrifugation at 1000*g* for 7 minutes at 4°C to remove nuclei and intact cells. The pellet was rehomogenized and spun again under the same conditions. The supernatants from the 2 low-speed spins were combined and centrifuged at 120,000*g* for 1 hour at 4°C. The pellet, containing the total membrane fraction, was suspended in 0.2 M KCl and 10 mM 4-(2-Hydroxyethyl)piperazine-1-ethanesulfonic acid (HEPES, pH 7.4). To solubilize the membrane fraction, an equal volume of 5% Triton X-100 and 10 mM HEPES (pH 7.4) was added to the sample, and the suspension was kept on ice for 1 hour. The unsolubilized material was pelleted by centrifugation at 10,000*g* for 10 minutes at 4°C, and the supernatant was analyzed by Western blot.

2.5.3. Surface protein biotinylation

Cell surface biotinylation was performed in DRG neurons as described in our previous study.[44] Briefly, the cultured DRG neurons were washed with cold PBS and then incubated in PBS containing 800 mg/mL Sulfo-NHS-LC-biotin (Pierce) for 45 minutes at 4°C to biotinylate surface proteins. After stopping the reaction with cold PBS containing 1 mM glycine, cells were lysed in buffer containing 0.1% Triton X-100, 0.1% SDS, 150 mM NaCl, 10 mM Tris-HCl (pH 7.4), and protease inhibitor cocktail (Roche). Cell debris was removed by centrifugation at 12,000 rpm for 10 minutes at 4°C. One hundred fifty micrograms of cell lysates were incubated with 30 μL immobilized NeutrAvidin Agarose (Pierce) at 4°C overnight. Then, agarose pellets were washed for 5 times in lysis buffer. Finally, biotinylated surface proteins were eluted from agarose beads by boiling at 95°C for 5 minutes in SDS sample buffer.

2.5.4. Western blot

Equal amounts of protein samples (20 μg) were denatured and then separated through SDS–polyacrylamide gel electrophoresis using 10% running gels and transferred to a polyvinylidene difluoride filter membrane (Bio-Rad, Hercules, CA). After blocking with 5% nonfat milk in Tris-buffered saline and Tween (TBST)

(20 mM Tris-HCl, pH 7.5, 150 mM NaCl, and 0.05% Tween-20) for 60 minutes at room temperature, the membrane was, respectively, incubated with the following primary antibodies at 4°C overnight: rabbit anti-rat IL-6 (1:300, Sigma-Aldrich), rabbit anti-rat IL-6R (1:500, Santa Cruz Biotechnology), rabbit anti-rat gp130 (1:500, Santa Cruz Biotechnology), rabbit anti-rat TRPV1 (1:200, Santa Cruz Biotechnology), rabbit anti-AKT (1:1000, Cell signaling Technology), rabbit anti–phosphorylated-AKT (Ser473) (1:1000, Cell signaling Technology), mouse anti-rat transferrin receptor (TfR, 1:1000, Life Technologies), and mouse anti-rat β-actin (1:2000, Santa Cruz Biotechnology). The blots were washed in TBST and then were incubated in horseradish peroxidase–conjugated goat anti-rabbit/mouse IgG secondary antibody (Santa Cruz Biotechnology). Protein bands were visualized using an enhanced chemiluminescence detection kit (Pierce) followed by autoradiography using Hyperfilm MP (Santa Cruz Biotechnology). The standardized ratio of IL-6, sIL-6R, gp130, or total TRPV1 to β-actin band density, or membrane TRPV1 to transferrin receptor, was used to calculate the alteration of corresponding protein expression.

2.6. Reverse transcription polymerase chain reaction and quantitative real-time polymerase chain reaction assay

Total RNA was extracted with TRIzol reagent (Life Technologies) according to the manufacturer's instructions. RNA (1 μg) was used for reverse transcription with MMLV reverse transcriptase (Takara, Tokyo, Japan). Template (1 μL) was amplified by polymerase chain reaction (PCR) with Taq DNA polymerase (Takara) in 25 μL total reaction volume containing 0.5 μM PCR primer as indicated. Polymerase chain reaction amplification consisted of 30 seconds at 94°C, 45 seconds at 56°C, and 30 seconds at 72°C for 32 cycles. Polymerase chain reaction products were separated in 2% agarose gel, stained by ethidium bromide, and visualized under ultraviolet light.

Quantitative real-time PCR was performed on an ABI 7500 Fast Real-Time PCR System (Applied Biosystems, Foster City, CA) with SYBR Premix Ex Taq II (Takara). In brief, a 20-μL PCR reaction was used that included 10 mM Tris-HCl (pH 8.3), 50 mM KCl, 2 mM $MgCl_2$, 200 μM dNTPs, 1.5 IU Taq DNA polymerase (Takara), 0.4 × SYBR Green 1 (Invitrogen), and 0.15 μM of each primer. β-actin in parallel for each run was used as an internal control. A 4-step experimental run protocol was used, and the amplification conditions were as follows: 95°C for 10 minutes (initial denaturation), 35 cycles of 25 seconds at 95°C (denaturation), 45 seconds at annealing temperature, 30 seconds at 72°C (elongation), and 8 seconds at fluorescence measurement temperature (60°C). Relative quantification of the expression of genes was calculated using the $2^{-(\Delta\Delta Ct)}$ method, where the Ct value is the cycle number at which the fluorescence signal crosses the threshold. The ΔCt was the difference between the PCR product and its internal control (β-actin). The ΔΔCt was the difference between the naive group and the other 2 groups. Data are expressed as $2^{-(\Delta\Delta Ct)}$, that is, the fold change in IL-6R, gp130, or TRPV1 mRNA.

The following primers were used for reverse transcription or real-time PCR reactions: IL-6R, 5′-ATGGACTACCACGGGAAACAC-3′ (forward) and 5′-TTGGATGCCACTCACAAAAGG-3′ (reverse); gp130, 5′-TCAACTTGTGGAACCATGTGG-3′ (forward) and 5′-TCCAACTGACACAGCATGTTC-3′ (reverse); TRPV1, 5′-GACATGCCACCCAGCAGG-3′ (forward) and 5′-TCAATTCCCACACACCTCCC-3′ (reverse); β-actin, 5′-AGCCATGTACGTAGCCATCC-3′ (forward) and 5′-GCCATCTCTTGCTCGAAGTC-3′ (reverse).

2.7. Whole-cell patch-clamp recordings

Whole-cell patch-clamp recordings were performed on acutely dissociated DRG neurons at room temperature using an EPC-10 amplifier with Patch-Master software (HEKA, Freiburg, Germany). Patch pipettes were pulled from borosilicate glass capillaries with a tip resistance of 5 to 8 MΩ when filled with an internal solution containing (in millimoles) 100 KCl, 10 ethylene glycol tetraacetic acid (EGTA), 40 HEPES, 5 $MgCl_2$, and 1 Na_2ATP, adjusted to pH 7.3 with KOH. The external solution contained (in millimoles) 128 NaCl, 5.4 KCl, 1.8 $CaCl_2$, 5 $MgCl_2$, 5.55 glucose, and 20 HEPES, adjusted to pH 7.4 with NaOH. Drugs were prepared in the external solution and delivered by a RSC-200 rapid solution changer system (Bio-Logic Science Instruments, Grenoble, France). Membrane currents and voltage were measured with both pipette and membrane capacitance cancellation, filtered at 2 kHz, and digitized at 10 kHz. Resting membrane potential (RMP) was measured immediately after rupture of the cell membrane in whole-cell patch mode.

Under current-clamp recording, the cells were held at 0 pA, and the firing threshold of DRG neurons was first measured by a series of 100-millisecond depolarizing current injection in 5-pA steps from 0 pA to elicit the first action potential (AP). To further examine the firing properties of neurons, a large depolarizing current of 500 milliseconds and 300 pA was delivered to the cell to ensure that all recorded neurons could be evoked sufficient firing, and the evoked discharges were elicited under an equal depolarizing current pulse.[81,82] We have demonstrated that this depolarizing current pulse (500 milliseconds, 300 pA) could evoke AP firing in all recorded DRG neurons in our preliminary experiments. In this study, we measured RMP, rheobase, threshold of AP (TP), and frequency of AP to evaluate intrinsic electrophysiological properties of cells.

Under voltage-clamp recording, cells were clamped at −70 mV, and series resistance was compensated from 70% to 90%. The membrane capacitance was read from the amplifier by Patch-Master software (HEKA) for determining the size of cells and calculating the current density. In this study, we applied capsaicin-evoked TRPV1 current for the identification of nociceptive DRG neurons in all electrophysiological experiments, and only the neurons expressing TRPV1 current were used for further statistical analyses. The agonist-evoked TRPV1 currents were measured by application of capsaicin (CAP, 0.5 μM for 3 seconds) to each recorded cells. Origin software 8.5 (OriginLab Corporation, Northampton, MA) was used for data analysis.

2.8. Statistical analysis

Statistical analyses were performed with GraphPad Prism 5 for Windows (GraphPad Software, La Jolla, CA). All data are expressed as mean ± SEM. A 2-tailed unpaired *t* test was used for the comparison of the mean values between 2 groups. One-way analysis of variance (ANOVA) followed by Dunnett multiple comparison test or 2-way ANOVA followed by Bonferroni post hoc test was used for multiple comparison. Differences with $P < 0.05$ were considered statistically significant.

3. Results

3.1. Upregulation of IL-6 and its receptors in the dorsal root ganglia of bone cancer rats

Production of IL-6 after bone destruction or nerve injury has been found in both patients with rheumatoid arthritis and neuropathic rats.[1,76] To determine whether IL-6 plays a role in the

development of bone cancer pain, we first examined the alteration of IL-6 in the DRG of bone cancer rats using Western blot assay. As shown in **Figure 1A**, expression of IL-6 in ipsilateral L4 and L5 DRG was statistically increased from day 7 (1.12 ± 0.06 MRMT-1 vs 0.79 ± 0.08 sham, $P < 0.01$) to day 21 (1.19 ± 0.05 MRMT-1 vs 0.96 ± 0.06 sham, $P < 0.05$) in MRMT-1 rats compared with sham rats (2-way ANOVA, n = 6).

It is well known that IL-6 exerts its biological effect on target cells either through classic signaling by binding to mIL-6R or through trans-signaling by binding to sIL-6R, thereafter inducing homodimerization of gp130 as a common signal transduction receptor.[65] We hence explored whether these IL-6 receptors (IL-6R) were expressed in rat DRG using reverse transcription PCR and Western blot approaches. We found that the expression of IL-6R mRNA was almost not detectable either in naive or in sham rat DRG, whereas in MRMT-1 rat DRG as well as in a positive control of the liver tissue, high expression of IL-6R mRNA was clearly observable (**Fig. 1B-a**). Moreover, we discovered that soluble IL-6 receptor (sIL-6R) but not membrane-bound IL-6 receptor (mIL-6R) was detected in the DRG among naive, sham,

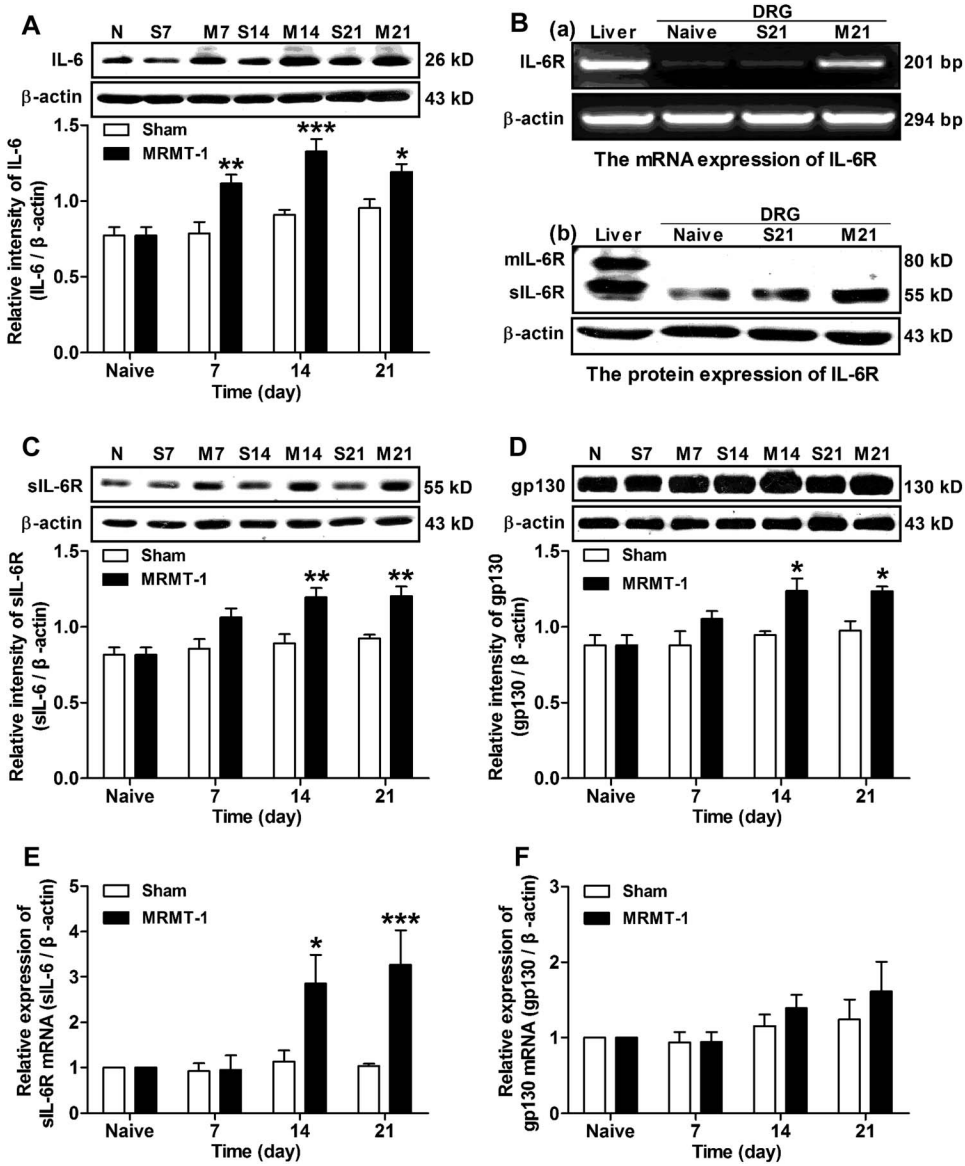

Figure 1. Expression of interleukin-6 (IL-6) and IL-6 receptors in the dorsal root ganglia (DRG) of bone cancer rats. (A), Western blot of IL-6 expression in ipsilateral L4 and L5 DRG. Upper: representative of Western blot bands; lower: analysis of the relative intensity of IL-6. β-actin is used as an internal control. Note that the expression of IL-6 is increased significantly from day 7 to day 21 in mammary rat metastasis tumor (MRMT-1) rats compared with sham rats. $^{*}P < 0.05$, $^{**}P < 0.01$, $^{***}P < 0.001$, 2-way analysis of variance (ANOVA), n = 6 per group. (B), Detection of IL-6 receptor (IL-6R) expression in DRG lysate in naive, sham, and MRMT-1 rats. (a), Reverse transcription polymerase chain reaction analysis of IL-6R mRNA expression. Note that the level of IL-6R mRNA is markedly increased in MRMT-1 rats compared with naive and sham rats. Liver tissue is used as a positive control. (b), Western blot of IL-6R protein expression. Note that the IL-6R protein is detected only in the form of soluble receptor in all rat DRG, whereas as a positive control, the liver tissue expresses both membrane-bound (mIL-6R) and soluble IL-6 receptors (sIL-6R) in naive rats. n = 3 per group. (C and D), Western blot of sIL-6R (C) and gp130 (D) expression in ipsilateral L4 and L5 DRG in naive, sham, and MRMT-1 rats. Note that the expression of both sIL-6R (C) and gp130 (D) are statistically increased from day 14 to day 21 in MRMT-1 rats compared with sham rats. $^{*}P < 0.05$, $^{**}P < 0.01$, 2-way ANOVA, n = 7 per group. (E and F), Quantitative real-time polymerase chain reaction assay of IL-6R mRNA (E) and gp130 mRNA (F) expression in ipsilateral L4 and L5 DRG in naive, sham, and MRMT-1 rats. Note that the expression of IL-6R mRNA but not the gp130 mRNA is prominently increased from day 14 to day 21 in MRMT-1 rats compared with sham rats. $^{*}P < 0.05$, $^{***}P < 0.001$, 2-way ANOVA, n = 5 to 6 per group. M, MRMT-1; N, naive; S, sham.

and MRMT-1 rats, while as positive controls, both forms of IL-6R (ie, mIL-6R and sIL-6R) could be detected in the liver tissue (**Fig. 1B-b**). These results suggest that IL-6 plays its roles in the DRG likely through trans-signaling by binding to sIL-6R.

Furthermore, we investigated the changes of sIL-6R and the common signal transduction receptor gp130 in the DRG of bone cancer rats. Using Western blot assay, we found that the expression of sIL-6R protein in ipsilateral L4 and L5 DRG was remarkably increased from day 14 (1.19 ± 0.08 MRMT-1 vs 0.95 ± 0.03 sham, $P < 0.01$) to day 21 (1.20 ± 0.06 MRMT-1 vs 0.93 ± 0.02 sham, $P < 0.01$) in MRMT-1 rats in contrast to sham rats (2-way ANOVA, n = 7) (**Fig. 1C**). Similarly, the expression of gp130 protein was also markedly increased from day 14 (1.24 ± 0.08 MRMT-1 vs 0.95 ± 0.03 sham, $P < 0.05$) to day 21 (1.24 ± 0.03 MRMT-1 vs 0.98 ± 0.06 sham, $P < 0.05$) in MRMT-1 rats compared with sham rats (2-way ANOVA, n = 7) (**Fig. 1D**). Additionally, using quantitative real-time PCR assay, we observed that in line with its protein expression, the IL-6R mRNA level was also dramatically increased from day 14 (2.85 ± 0.64 MRMT-1 vs 1.14 ± 0.24 sham, $P < 0.05$) to day 21 (3.27 ± 0.76 MRMT-1 vs 1.03 ± 0.05 sham, $P < 0.001$) in MRMT-1 rats in contrast to sham rats (2-way ANOVA, n = 5) (**Fig. 1E**). Unexpectedly, no significant difference was found in gp130 mRNA expression between the MRMT-1 rats and the sham rats ($P > 0.05$, 2-way ANOVA, n = 6) (**Fig. 1F**).

3.2. FIL-6 induces overexcitability of nociceptive dorsal root ganglion neurons and pain hypersensitivity in normal rats

To investigate whether increased IL-6 and sIL-6R contributed to the pathogenesis of bone cancer–induced pain, we first evaluated the effects of extraneous application of FIL-6 (a mixture of IL-6 [50 ng/mL] together with sIL-6R [50 ng/mL] that has been widely used in previous studies[31,32,67]) on excitability of nociceptive DRG neurons and pain behaviors in normal rats. Using whole-cell patch-clamp recording techniques, we found that FIL-6 could induce overexcitability of nociceptive DRG neurons acutely isolated from normal rats. The nociceptive DRG neurons were identified by capsaicin (CAP, 0.5 μM for 3 seconds)-evoked TRPV1 current as described in the Methods section. As shown in **Figures. 2A-B**, after incubating the cells with FIL-6 (50 ng/mL) for 10 minutes, the discharge frequency (spikes per 500 milliseconds) of TRPV1 current–positive DRG neurons (named as nociceptive DRG neurons in the following text) evoked by a 500-millisecond 300 pA depolarizing current was remarkably increased in the FIL-6-treated group (12.42 ± 2.24, n = 20) as compared with the vehicle PBS-treated group (3.86 ± 0.85, n = 21) ($P < 0.01$, 1-way ANOVA). As expected, the effect of FIL-6 on spike frequency of DRG neurons was almost completely blocked by sgp130 (50 ng/mL), a potent inhibitor of IL-6/sIL-6R complex that has been widely used for the blockade of IL-6/sIL-6R trans-signaling pathway[10,12,32,65] (5.78 ± 1.99 sgp130 + FIL-6 vs 12.42 ± 2.24 FIL-6, $P < 0.05$, 1-way ANOVA, n = 18: sgp130 + FIL-6 and 20: FIL-6, **Fig. 2B**).

Moreover, we examined the following intrinsic properties of nociceptive DRG neurons including rheobase (the minimal current pulse required for triggering an AP), RMP, and TP (the voltage threshold for triggering an AP), which are well known to be associated with neuronal excitability. We found that all these intrinsic electrogenic properties of nociceptive DRG neurons were prominently altered after the treatment of FIL-6 to DRG neurons (**Figs. 2C–F**). For instance, in contrast to the control PBS-treated cells, the FIL-6-treated nociceptive DRG neurons showed more depolarized RMP (−46.11 ± 0.97 mV FIL-6 vs −51.90 ± 1.55 mV PBS, $P < 0.01$, n = 18 FIL-6 and 20 PBS, 1-way ANOVA, **Figs. 2C and E**), more decreased rheobase (169.72 ± 12.78 pA FIL-6 vs 227.62 ± 21.12 pA PBS, $P < 0.05$, n = 18 FIL-6 and 21 PBS, 1-way ANOVA, **Figs. 2C-D**), and more declined TP (−14.95 ± 0.59 mV FIL-6 vs −9.98 ± 0.57 mV PBS, $P < 0.001$, n = 18 FIL-6 and 20 PBS, 1-way ANOVA, **Figs. 2C and F**). Similarly, all these effects of FIL-6 on the intrinsic electrogenic properties of nociceptive DRG neurons were robustly blocked by sgp130 (50 ng/mL), a potent inhibitor of IL-6/sIL-6R complex ($P < 0.05$-0.001, sgp130 + FIL-6 vs FIL-6, 1-way ANOVA, **Figs. 2C to F**).

In addition, the behavioral studies revealed that intrathecal administration of FIL-6 (100 ng/10-μL) produced both mechanical allodynia and thermal hyperalgesia in normal rats, and all these effects of FIL-6 could be blocked by its potent inhibitor sgp130 (100 ng/mL) (**Figs. 2G-H**). The ipsilateral PWT responding to von Frey filaments was significantly decreased in FIL-6-treated rats (5.35 ± 0.96*g* and 9.62 ± 1.44*g* at 1 hour and 24 hours postdrug, respectively) as compared with PBS-treated rats (14.32 ± 0.69*g* and 14.72 ± 0.29*g* at 1 hour and 24 hours postdrug, respectively, $P < 0.001$) or sgp130 + FIL-6-treated rats (11.73 ± 1.46*g* and 13.56 ± 0.74*g* at 1 hour and 24 hours postdrug, respectively, $P < 0.001$ and $P < 0.05$) (**Fig. 2G**). Similarly, the ipsilateral PWL responding to radiant heat stimuli also was markedly decreased in FIL-6-treated rats (9.94 ± 0.81 seconds and 11.19 ± 1.08 seconds at 1 hour and 24 hours postdrug, respectively) as compared with PBS-treated rats (14.88 ± 0.96 seconds and 15.01 ± 0.75 seconds at 1 hour and 24 hours postdrug, respectively, $P < 0.001$) or sgp130 + FIL-6-treated rats (13.58 ± 0.97 seconds and 14.57 ± 0.89 seconds at 1 hour and 24 hours postdrug, respectively, $P < 0.05$) (**Fig. 2H**). As evaluated by the inclined-plate test, no apparent motor dysfunction was observed after intrathecal administration of the above each drugs (data not shown). These data imply that extraneous application of FIL-6 induces alterations of intrinsic electrogenic properties of nociceptive DRG neurons through IL-6/sIL-6R trans-signaling pathway, thereby leading to overexcitability (ie, sensitization) of primary sensory neurons and pain hypersensitivity in normal rats.

3.3. Inhibition of IL-6/sIL-6R trans-signaling by sgp130 reduces dorsal root ganglion neurons hyperexcitability and attenuates pain hypersensitivity in bone cancer rats

To further validate whether or not the IL-6/sIL-6R trans-signaling is involved in the development of bone cancer–induced pain through the induction of DRG neurons hyperexcitability in bone cancer rats, we investigated the effects of both pretreatment and posttreatment with sgp130, a potent IL-6/sIL-6R trans-signaling inhibitor, on DRG neurons excitability and pain behaviors in bone cancer rats. As shown in **Figures 3A–D**, pretreatment with sgp130 (100 ng/10 μL, once per day from day 7 to day 13 after inoculation surgery) could significantly prevent the bone cancer–induced hyperexcitability of DRG neurons and pain hypersensitivity in MRMT-1 rats. The bone cancer–induced increase in spike numbers of AP evoked by a 500-millisecond 300 pA depolarizing current pulse was prominently inhibited in MRMT-1 + sgp130 rats (2.92 ± 1.15, n = 24) compared with MRMT-1 + PBS rats (9.45 ± 2.14, n = 20) ($P < 0.01$, 1-way ANOVA, **Fig. 3B**). Similarly, the bone cancer–induced decreases in both PWT and PWL were also dramatically prevented in MRMT-1 + sgp130 rats (PWT: 11.86 ± 1.00*g*, n = 7; PWL: 13.43 ± 0.85 seconds, n = 8) compared with MRMT-1 + PBS rats (PWT: 5.30 ± 0.71*g*, n = 6; PWL: 8.90 ± 0.43 seconds, n = 7) ($P < 0.001$, 1-way ANOVA,

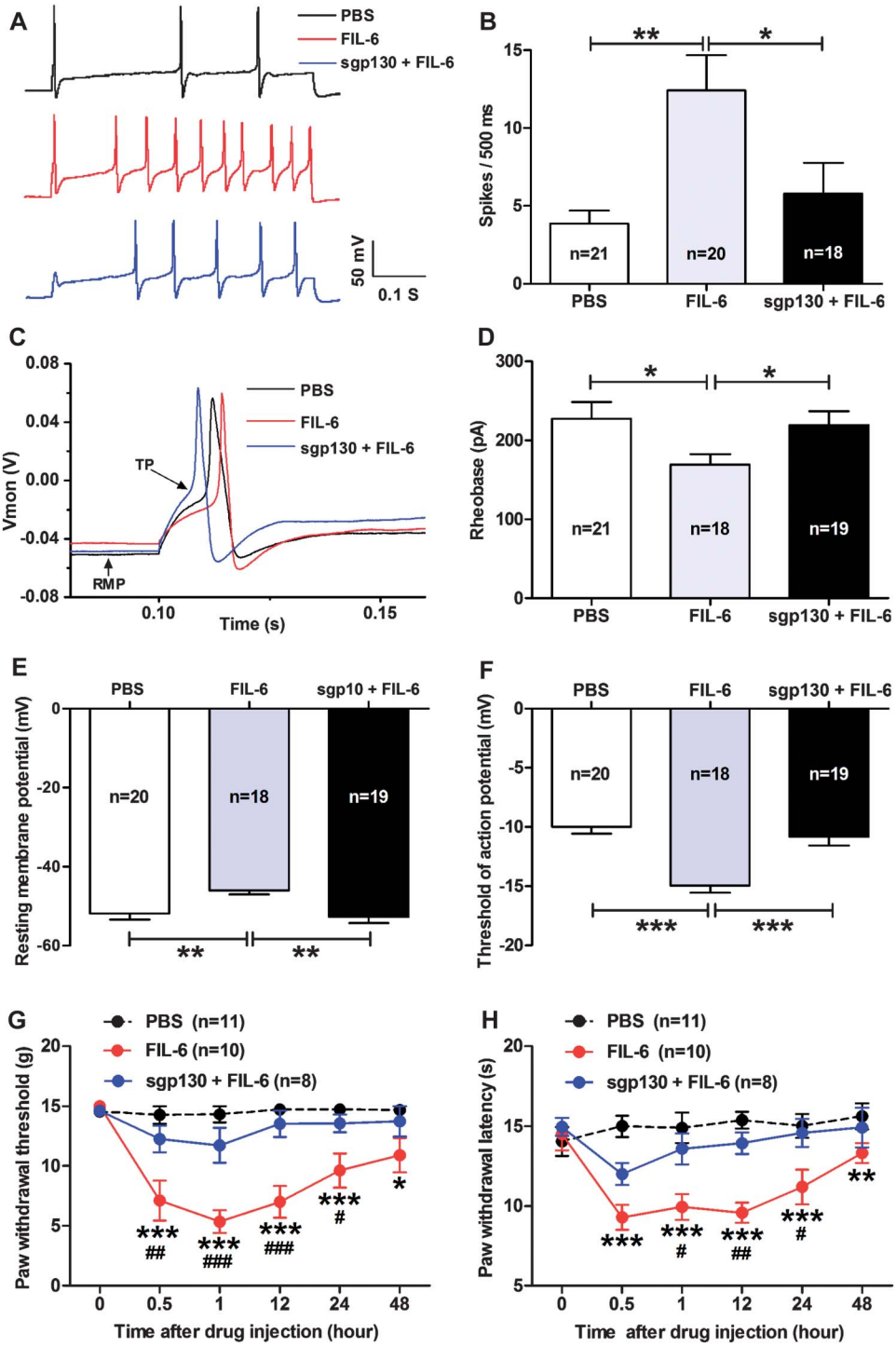

Figure 2. FIL-6 induces both neuronal hyperexcitability in acutely dissociated dorsal root ganglion (DRG) neurons and pain hypersensitivity in normal rats. (A), Representative traces of action potential (AP) discharges evoked by a 500-millisecond 300 pA depolarizing current pulse delivered to phosphate-buffered saline (PBS)–, FIL-6-, and sgp130 + FIL-6–treated DRG neurons. Scale bar: 50 mV, 0.1 seconds. (B), Analysis of the evoked AP numbers. Note that the number of the evoked AP is significantly increased in the FIL-6-treated group compared with the PBS-treated group, while sgp130 blocks all these actions of FIL-6. $^{*}P < 0.05$, $^{**}P < 0.01$, 1-way analysis of variance (ANOVA), n = 21 (PBS), 20 (FIL-6), and 18 (sgp130 + FIL-6). (C), Representative traces of the first AP evoked by a series of step depolarizing current (100 milliseconds, in 5-pA steps from 0 pA) delivered to PBS-, FIL-6- and sgp130 + FIL-6–treated DRG neurons. (D–F), Summary of the rheobase (D), the resting membrane potential (E), and the threshold of AP (TP) (F). Note that the rheobase is decreased and the TP is declined, while the resting membrane potential is more depolarized in FIL-6-treated neurons compared with PBS-treated neurons, and the sgp130 almost completely blocks all these actions of FIL-6. $^{*}P < 0.05$, $^{**}P < 0.01$, $^{***}P < 0.001$, 1-way ANOVA, n = 20 (PBS), 18 (FIL-6), and 19 (sgp130 + FIL-6). (G and H), Effects of intrathecal administration of FIL-6 or sgp130 plus FIL-6 on the mechanical allodynia (G) and thermal hyperalgesia (H) of normal rats. Note that FIL-6 induces a significant decrease both in the paw withdrawal threshold and the paw withdrawal latency compared with the vehicle group, and sgp130 dramatically blocks the FIL-6-induced mechanical allodynia and thermal hyperalgesia. $^{*}P < 0.05$, $^{**}P < 0.01$, $^{***}P < 0.001$, compared with the PBS group; $^{*}P < 0.05$, $^{**}P < 0.01$, $^{***}P < 0.01$, compared with the sgp130 + FIL-6 group, 2-way ANOVA, n = 11 (PBS), 10 (FIL-6), and 8 (sgp130 + FIL-6).

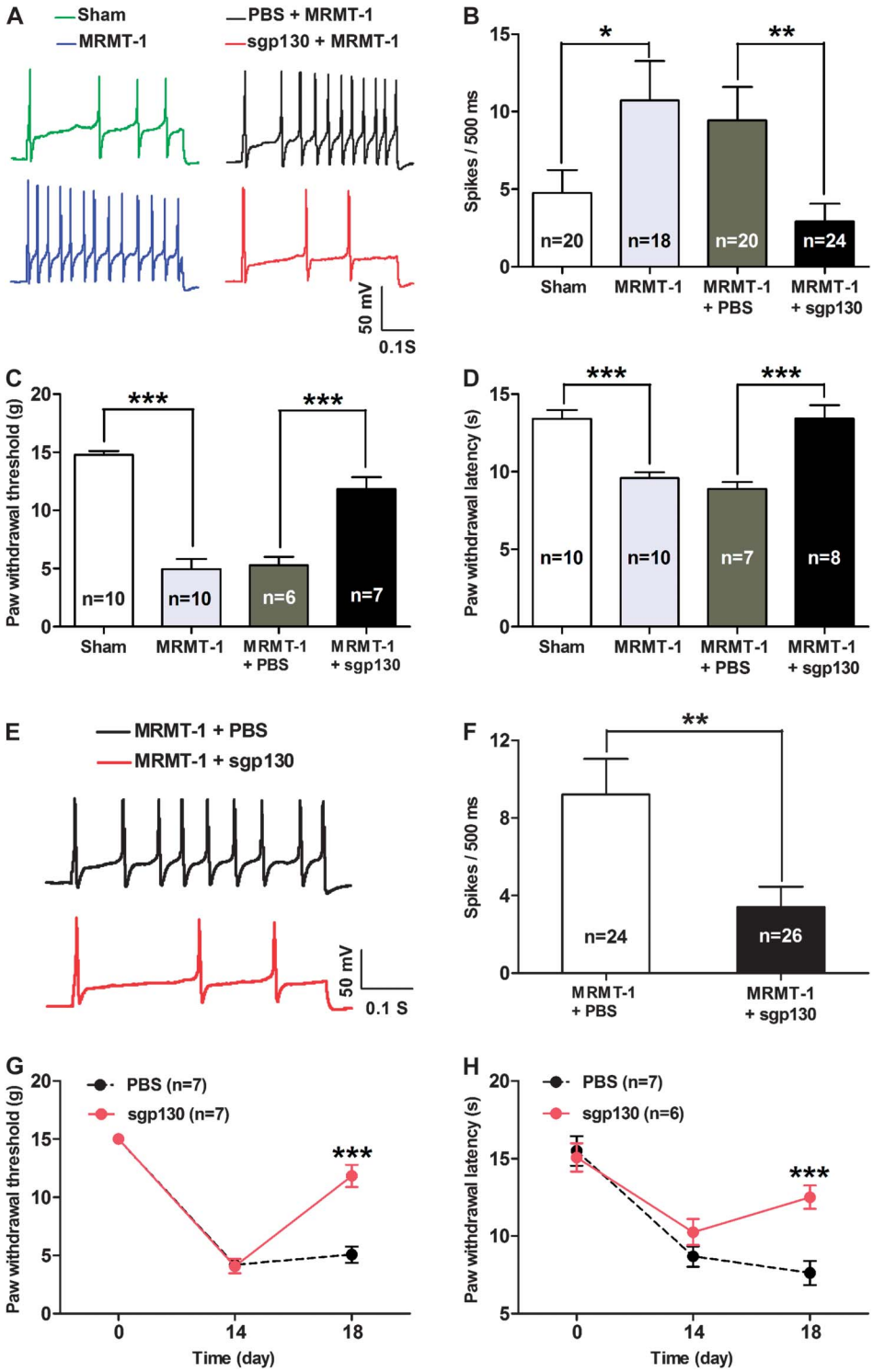

Figure 3. Effects of pretreatment or posttreatment with sgp130 on dorsal root ganglion (DRG) neuron hyperexcitability and pain hypersensitivity in bone cancer rats. (A and B), Effects of pretreatment with sgp130 on DRG neuron excitability. (A), Representative traces of action potential (AP) discharges evoked by a 500-millisecond 300 pA depolarizing current pulse delivered to acutely dissociated DRG neurons. Scale bar: 50 mV, 0.1 seconds. (B), Analysis of the evoked AP numbers. Note that the number of the evoked AP is significantly increased in the mammary rat metastasis tumor (MRMT-1) group compared with the sham group, while pretreatment with sgp130 remarkably inhibits the bone cancer–induced hyperexcitability of DRG neurons. $^{*}P < 0.05$, $^{**}P < 0.01$, 1-way analysis of variance (ANOVA), n = 20 (sham), 18 (MRMT-1), 20 (MRMT-1 + phosphate-buffered saline [PBS]), and 24 (MRMT-1 + sgp130). (C and D), Effects of pretreatment with sgp130 on the mechanical allodynia (C) and thermal hyperalgesia (D) of MRMT-1 rats. Note that both the paw withdrawal threshold and paw withdrawal latency are statistically decreased in MRMT-1 rats compared with sham rats, while sgp130 can prominently block all these decreases. $^{***}P < 0.001$, 1-way ANOVA, n = 6 to 10 per group. (E and F), Effects of posttreatment with sgp130 on DRG neuron excitability. (E), Representative traces of AP discharges evoked by a 500-millisecond 300 pA depolarizing current pulse delivered to acutely dissociated DRG neurons. (F), Analysis of the evoked AP numbers. Note that posttreatment with sgp130 significantly inhibits the bone cancer–induced hyperexcitability of cancer rat DRG neurons. $^{**}P < 0.01$, 2-tailed unpaired *t* test, n = 24 (MRMT-1 + PBS) and 26 (MRMT-1 + sgp130). (G and H), Effects of posttreatment with sgp130 on the mechanical allodynia (C) and thermal hyperalgesia (D) of MRMT-1 rats. Note that posttreatment with sgp130 can markedly restore the bone cancer–induced decreases in both paw withdrawal threshold and paw withdrawal latency. $^{***}P < 0.001$, 2-way ANOVA, n = 6 (PBS) and 7 (sgp130).

Figs. 3C-D). Meanwhile, we found that posttreatment with sgp130 (100 ng/10 μL, once per day from day 15 to day 17 after inoculation surgery) could attenuate the bone cancer–induced hyperexcitability of DRG neurons and the bone cancer–induced pain hypersensitivity in MRMT-1 rats (**Figs. 3E-H**). For instance, the bone cancer–induced increase in evoked discharges was markedly inhibited in MRMT-1 + sgp130 rats (3.40 ± 1.05, n = 26) compared with MRMT-1 + PBS rats (9.21 ± 1.84, n = 24) ($P < 0.01$, 1-way ANOVA, **Fig. 3F**). Accordantly, the bone cancer–induced decreases in both PWT and PWL were also obviously restored in MRMT-1 + sgp130 rats (PWT: 11.84 ± 0.95*g*, n = 7; PWL: 12.51 ± 0.75 seconds, n = 6) compared with MRMT-1 + PBS rats (PWT: 5.07 ± 0.71*g*, n = 7; PWL: 7.62 ± 0.78 seconds, n = 7) ($P < 0.001$, 1-way ANOVA, **Figs. 3G-H**). These results demonstrate that inhibition of IL-6/sIL-6R trans-signaling by sgp130 suppresses the bone cancer–induced hyperexcitability of DRG neurons and pain hypersensitivity in MRMT-1 rats, implying that the IL-6/sIL-6R trans-signaling is involved in the pathogenesis of bone cancer–induced pain through the induction of DRG neurons hyperexcitability in bone cancer rats.

3.4. FIL-6 induces functional upregulation of TRPV1 in dorsal root ganglion neurons through the activation of JAK/PI3K signaling pathway, which is involved in FIL-6-mediated pain hypersensitivity in normal rats

To determine the downstream target on which the enhanced IL-6 in DRG neurons exerts its effects for the development of bone cancer pain, we focused on TRPV1, a transient receptor potential vanilloid channel type 1, that can be potentiated by IL-6/gp130 ligand receptor complex[2,58] and is well documented to be involved in the pathogenesis of various persistent pain.[8,33,42,60,68] First, we investigated whether IL-6 could induce a functional upregulation of TRPV1 in DRG neurons by examining both short-term and long-term effects of IL-6 on expression of TRPV1 protein and mRNA as described in a previous report.[74] As shown in **Figure 4**, long-term (6-48 hours) rather than short-term (10-90 minutes) exposure of cultured DRG neurons to FIL-6, a mixture of IL-6/sIL-6R (50 ng/mL), produced a significant increase in the expression of TRPV1 total protein. For example, the relative intensity of TRPV1 total protein was statistically increased at 6 hours (1.19 ± 0.06, $P < 0.01$), 12 hours (1.29 ± 0.05, $P < 0.001$), and 24 hours (1.03 ± 0.09, $P < 0.05$) after the incubation of FIL-6 as compared with PBS (0.76 ± 0.06) (1-way ANOVA, n = 5, **Fig. 4B**), whereas the expression of TRPV1 total protein was not significantly changed after short-term (up to 90 minutes) exposure of DRG neurons to FIL-6 in contrast to PBS ($P > 0.05$, 1-way ANOVA, n = 6, **Fig. 4A**). Moreover, we found that the FIL-6-induced increase in TRPV1 total protein (1.29 ± 0.08) after long-term (12 hours) exposure of DRG neurons to FIL-6 was almost completely blocked in the presence of anisomycin (50 μM), a general protein synthesis inhibitor (0.83 ± 0.08) ($P < 0.01$, 1-way ANOVA, n = 4, supplementary data, Figs. S4A and 4B available online as Supplemental Digital Content at http://links.lww.com/PAIN/A65), indicating that the long-term effects of FIL-6 on the upregulation of TRPV1 total protein are probably dependent on nascent protein synthesis through translational regulation. However, no significant alteration was observed on TRPV1 mRNA expression either after short-term or after long-term exposure of DRG neurons to FIL-6 in contrast to PBS ($P > 0.05$, 1-way ANOVA, n = 6, **Figs. 4C-D**). These results raise the possibility that the increased expression of TRPV1 total protein in DRG neurons after long-term treatment with FIL-6 likely occurs through a translational rather than a transcriptional mechanism.

It is well known that the binding of IL-6 to its signal transducing receptor gp130 can activate downstream JAK/STAT, MAPK/ERK, and PI3K/AKT signaling pathways.[20] To identify which of the signaling pathways is involved in FIL-6-mediated upregulation of TRPV1 total protein in DRG neurons, the effects of sgp130 (50 ng/mL, an IL-6/sIL-6R trans-signaling inhibitor), AG490 (20 μM, a JAK inhibitor), PD98059 (20 μM, a MEK inhibitor), and LY294002 (20 μM, a PI3K inhibitor) on FIL-6-induced expression of TRPV1 total protein were evaluated in cultured DRG neurons, respectively. The results showed that when cultured DRG neurons were pretreated with the sole inhibitor for 10 minutes followed by cotreatment with FIL-6 (50 ng/mL) for 12 hours, the FIL-6-induced increase in expression of TRPV1 total protein could be dramatically blocked by each of these inhibitors (**Figs. 4E-F**). The relative intensity of TRPV1 total protein was statistically decreased in the sgp130 + FIL-6 group (0.99 ± 0.06) as compared with the PBS + FIL-6 group (1.32 ± 0.05) ($P < 0.01$, 1-way ANOVA, n = 6, **Fig. 4E**). Similarly, the expression of TRPV1 total protein was also remarkably reduced in the AG490 + FIL-6 group (0.97 ± 0.07), the PD98059 + FIL-6 group (0.93 ± 0.08), and the LY294002 + FIL-6 group (0.97 ± 0.03) in contrast to the DMSO + FIL-6 group (1.22 ± 0.04), respectively ($P < 0.05$, 1-way ANOVA, n = 5, **Fig. 4F**). These data indicate that both the MAPK/ERK and the PI3K/AKT signaling pathways are activated by FIL-6 for regulating TRPV1 total protein expression in DRG neurons. As to the JAK/STAT pathway, it is well known that JAK functions to phosphorylate STAT and promote its nuclear transfer and transcriptional function.[9,20] However, in this study we found that the TRPV1 mRNA level was not significantly altered either after short-term or after long-term exposure of DRG neurons to FIL-6. We reasoned that the JAK/STAT pathway is not involved in the FIL-6-mediated increase of TRPV1 total protein expression. Therefore, JAK probably promotes the expression of TRPV1 total protein through other novel pathways.

Considering the functional significance of membrane TRPV1, we further examined both the short-term and long-term effects of FIL-6 on membrane TRPV1 protein expression in cultured DRG neurons. Unlike TRPV1 total protein, we found that both short-term (10-90 minutes) and long-term (6-48 hours) exposure of cultured DRG neurons to FIL-6 (50 ng/mL) could produce a prominent increase in expression of TRPV1 membrane protein (**Fig. 5**). The relative intensity of TRPV1 membrane protein was statistically increased from 10 minutes to 90 minutes (1.05 ± 0.07 FIL-6 at 10 minutes and 1.09 ± 0.06 FIL-6 at 90 minutes vs 0.74 ± 0.06 PBS, $P < 0.01$, n = 6, **Fig. 5A**) and from 6 hours to 24 hours (1.04 ± 0.06 FIL-6 at 6 hours and 1.13 ± 0.05 FIL-6 at 24 hours vs 0.79 ± 0.07 PBS, $P < 0.05$-0.01, n = 4, **Fig. 5B**) after short-term and long-term incubation of FIL-6 in contrast to PBS, respectively (1-way ANOVA). In addition, we found that anisomycin (50 μM), a general protein synthesis inhibitor, blocked the FIL-6-induced increase in membrane TRPV1 protein after a long-term (0.96 ± 0.03 FIL-6 + anisomycin vs 1.26 ± 0.04 FIL-6 + DMSO at 12 hours, $P < 0.01$) but not a short-term (1.12 ± 0.09 FIL-6 + anisomycin vs 1.15 ± 1.00 FIL-6 + DMSO at 30 minutes, $P > 0.05$) exposure of DRG neurons to FIL-6 (1-way ANOVA, n = 3, supplementary data, Figs. S4C and D available online as Supplemental Digital Content at http://links.lww.com/PAIN/A65).

With respect to the downstream signaling pathways, we found that all the following inhibitors of sgp130 (an IL-6/sIL-6R trans-signaling inhibitor), AG490 (a JAK inhibitor), PD98059 (a MEK inhibitor), and LY294002 (a PI3K inhibitor) could block the increased expression of TRPV1 membrane protein either after short-term or after long-term exposure of DRG neurons to FIL-6 ($P < 0.05$-0.001, vs DMSO, 1-way ANOVA, n = 4-6,

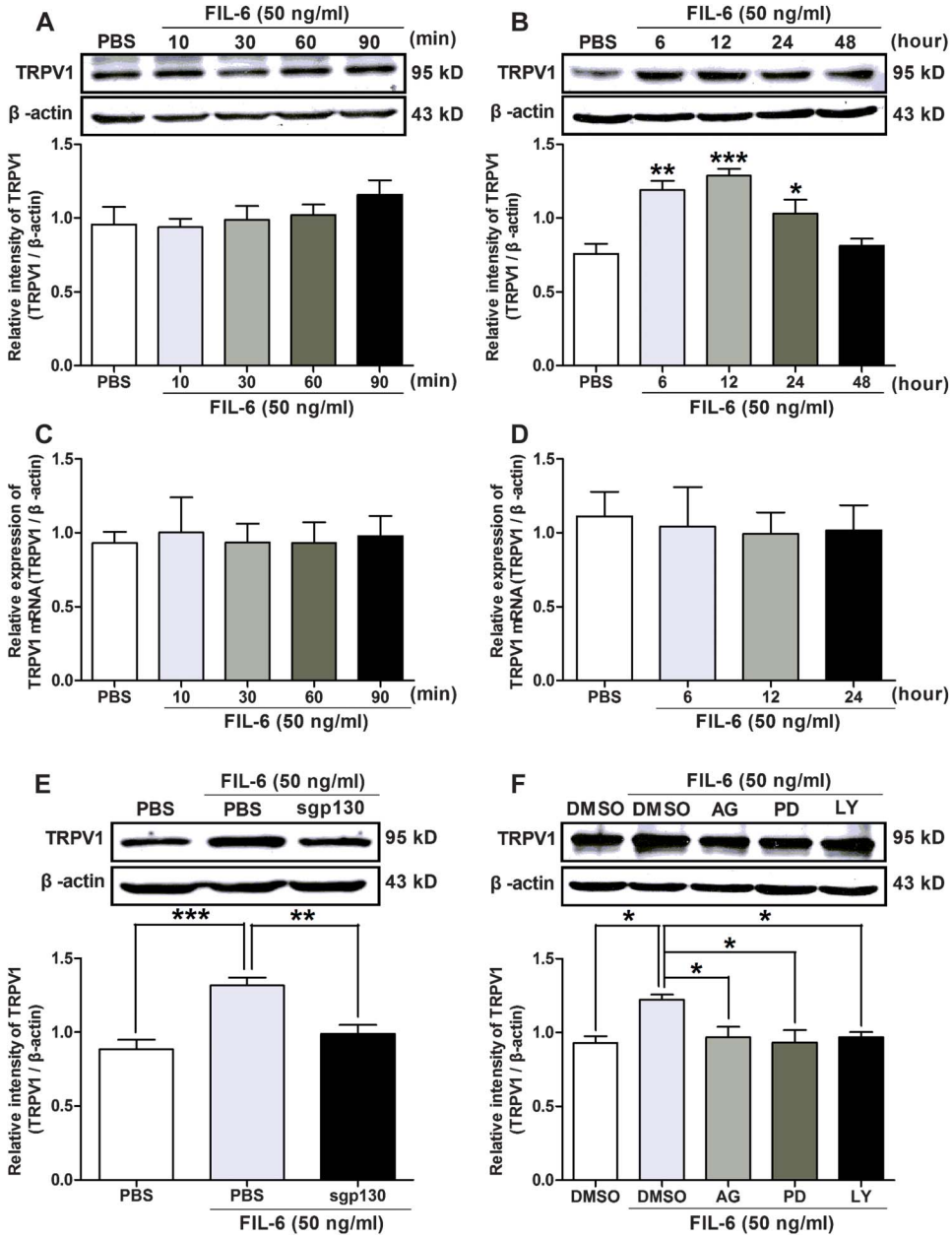

Figure 4. Short-term and long-term effects of FIL-6 on TRPV1 total protein and mRNA expression in cultured dorsal root ganglion (DRG) neurons. (A and B), Western blot of TRPV1 total protein expression in cultured DRG neurons after short-term (A) and long-term (B) treatment with FIL-6. Upper: representative of Western blot bands; lower: analysis of the relative intensity of TRPV1 total protein. β-actin is used as an internal control. Note that long-term (6-48 hours) rather than short-term (10-90 minutes) exposure of cultured DRG neurons to FIL-6 induces a significant increase in TRPV1 total protein expression. $^{*}P < 0.05$, $^{**}P < 0.01$, $^{***}P < 0.001$, compared with the phosphate-buffered saline group, 1-way analysis of variance (ANOVA), n = 5 to 6 per group. (C and D), Quantitative real-time polymerase chain reaction assay of TRPV1 mRNA expression in cultured DRG neurons after short-term (C) and long-term (D) treatment with FIL-6. Note that no significant alteration is observed on TRPV1 mRNA expression either after short-term or after long-term exposure of DRG neurons to FIL-6 in contrast to phosphate-buffered saline. $P > 0.05$, 1-way ANOVA, n = 7 to 8 per group. (E and F), Effects of sgp130 (an IL-6/sIL-6R trans-signaling inhibitor) (E) and AG490 (a JAK inhibitor), PD98059 (a MEK inhibitor) as well as LY294002 (a PI3K inhibitor) (F) on FIL-6-induced TRPV1 total protein expression. Upper: representative of Western blot bands; lower: analysis of the relative intensity of TRPV1 total protein. Note that all these inhibitors can significantly block the FIL-6-induced increase in TRPV1 total protein expression after long-term (12 hours) exposure of DRG neurons to FIL-6. $^{*}P < 0.05$, $^{**}P < 0.01$, $^{***}P < 0.001$, 1-way ANOVA, n = 5 to 6 per group.

Figs. 5C to F). As described in earlier section, the JAK/STAT pathway mainly functions for transcriptional regulation.[9,20] However, in this study, we found that JAK promotes membrane TRPV1 protein expression without the participation of transcriptional machinery. In a previous study, Yamada et al.[78] have reported that JAK kinase can activate PI3K cascade in adult T-cell leukemia cells; these findings thereby raise the possibility that JAK may promote membrane TRPV1 protein expression through the activation of PI3K cascade, which is involved in FIL-6-induced upregulation of membrane TRPV1 protein expression on cultured DRG neurons. To test this notion, we explored the cascade between JAK and PI3K by evaluating the effects of AG490 (a JAK inhibitor) on FIL-6-induced phosphorylation of AKT, a downstream effector of PI3K, in cultured DRG neurons. We discovered

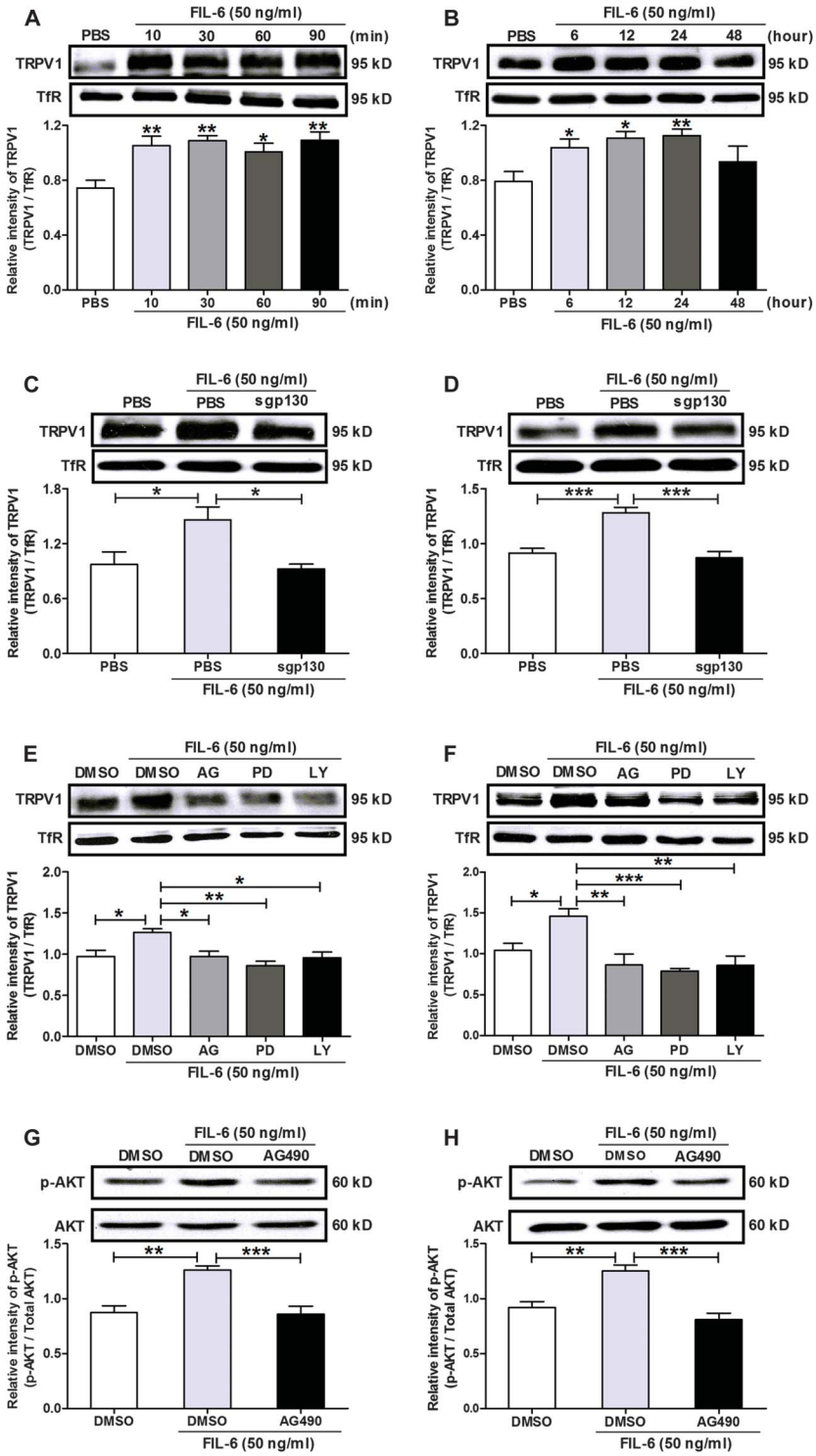

Figure 5. Short-term and long-term effects of FIL-6 on membrane TRPV1 protein expression in cultured dorsal root ganglion (DRG) neurons. (A and B), Western blot of membrane TRPV1 protein expression in cultured DRG neurons after short-term (A) and long-term (B) treatment with FIL-6. Upper: representative of Western blot bands; lower: analysis of the relative intensity of TRPV1 membrane protein. TfR (transferrin receptor) is used as an internal control. Note that both short-term (10-90 minutes) and long-term (6-48 hours) exposure of cultured DRG neurons to FIL-6 produce a prominent increase in the expression of TRPV1 membrane protein. $^{*}P < 0.05$, $^{**}P < 0.01$, compared with the phosphate-buffered saline group, 1-way analysis of variance (ANOVA), n = 4 to 6 per group. (C and D), Effects of sgp130 (an IL-6/sIL-6R trans-signaling inhibitor) on FIL-6-induced membrane TRPV1 protein expression in cultured DRG neurons. Note that sgp130 can significantly block the increased expression of TRPV1 membrane protein either after short-term (C) or after long-term (D) exposure of DRG neurons to FIL-6. $^{*}P < 0.05$, $^{***}P < 0.001$, 1-way ANOVA, n = 4 to 5 per group. (E and F), Effects of AG490 (a JAK inhibitor), PD98059 (a MEK inhibitor), and LY294002 (a PI3K inhibitor) on FIL-6-induced membrane TRPV1 protein expression in cultured DRG neurons. Note that all these inhibitors can remarkably block the increased expression of TRPV1 membrane protein either after short-term (E) or after long-term (F) exposure of DRG neurons to FIL-6. $^{*}P < 0.05$, $^{**}P < 0.01$, $^{***}P < 0.001$, 1-way ANOVA, n = 5 to 6 per group. (G and H), Effects of JAK inhibitor AG490 on FIL-6-induced expression of phosphorylated AKT (p-AKT) in cultured DRG neurons. Note that AG490 can dramatically block the FIL-6-induced increase of AKT phosphorylation either after short-term (G) or after long-term (H) exposure of DRG neurons to FIL-6. $^{**}P < 0.01$, $^{***}P < 0.001$, 1-way ANOVA, n = 5 to 6 per group.

that AG490 could significantly block the FIL-6-induced increase of AKT phosphorylation either after short-term or after long-term exposure of DRG neurons to FIL-6 (**Figs. 5G-H**). The relative intensity of phosphorylated AKT (p-AKT) was 0.86 ± 0.07 in the AG490 + FIL-6 group compared with 1.26 ± 0.04 in the DMSO + FIL-6 group ($P < 0.001$, n = 6, **Fig. 5G**) after short-term (30 minutes) exposure of DRG neurons to FIL-6 and was 0.81 ± 0.06 in the AG490 + FIL-6 group compared with 1.25 ± 0.05 in the DMSO + FIL-6 group ($P < 0.001$, n = 5, **Fig. 5H**) after long-term (12 hours) exposure of DRG neurons to FIL-6 (1-way ANOVA). These results imply that PI3K/AKT is a downstream target of JAK; thus, FIL-6 may promote membrane TRPV1 protein expression through the activation of JAK/PI3K signaling pathway, which is independent on JAK/STAT, a classical transcriptional regulatory pathway.

Next, we examined whether the FIL-6-induced increase of membrane TRPV1 on the DRG neurons is functional and whether activation of JAK/PI3K signaling pathway is involved in the FIL-6-mediated functional upregulation of TRPV1 and pain hypersensitivity in normal rats. As shown in **Figures 6A-B**, after long-term (12 hours) exposure of cultured DRG neurons to FIL-6 (50 ng/mL), the density of capsaicin (0.5 μM)-induced TRPV1 currents in the FIL-6 group (13.44 ± 2.20 pA/pF, n = 14) was significantly increased as compared with the PBS group (6.18 ± 0.61 pA/pF, n = 16, $P < 0.01$, 1-way ANOVA, **Fig. 6A**), and this FIL-6-induced potentiation of TRPV1 currents (in pA/pF) was markedly blocked by IL-6/sIL-6R trans-signaling inhibitor sgp130 (6.68 ± 1.67 in the sgp130 + FIL-6 group, n = 12 vs 13.44 ± 2.20 in the PBS + FIL-6 group, n = 14, $P < 0.05$, 1-way ANOVA, **Fig. 6A**), JAK inhibitor AG490 (4.73 ± 0.78 in the AG490 + FIL-6 group, n = 18), or PI3K inhibitor LY294002 (5.75 ± 0.98 in the LY294002 + FIL-6 group, n = 17) ($P < 0.01$-0.001, compared with the DMSO + FIL-6 group 12.05 ± 1.82, n = 19, 1-way ANOVA, **Fig. 6B**). Additionally, the behavioral studies revealed that JAK inhibitor AG490, PI3K inhibitor LY294002, or TRPV1 receptor antagonist capsazepine (CPZ) could remarkably block FIL-6-induced mechanical allodynia (**Fig. 6C**) and thermal hyperalgesia (**Fig. 6D**) in rats. For instance, 12 hours after drug administration, the FIL-6-induced decrease in PWT (6.95 ± 1.26 g, n = 10) was significantly restored by pretreatment with AG490 (11.86 ± 1.26*g*, $P < 0.05$, n = 9), LY294002 (13.20 ± 0.81*g*, $P < 0.001$, n = 9), or CPZ (13.22 ± 1.15*g*, $P < 0.01$, n = 8) (2-way ANOVA, **Fig. 6C**). Similarly, the FIL-6-induced decrease in PWL

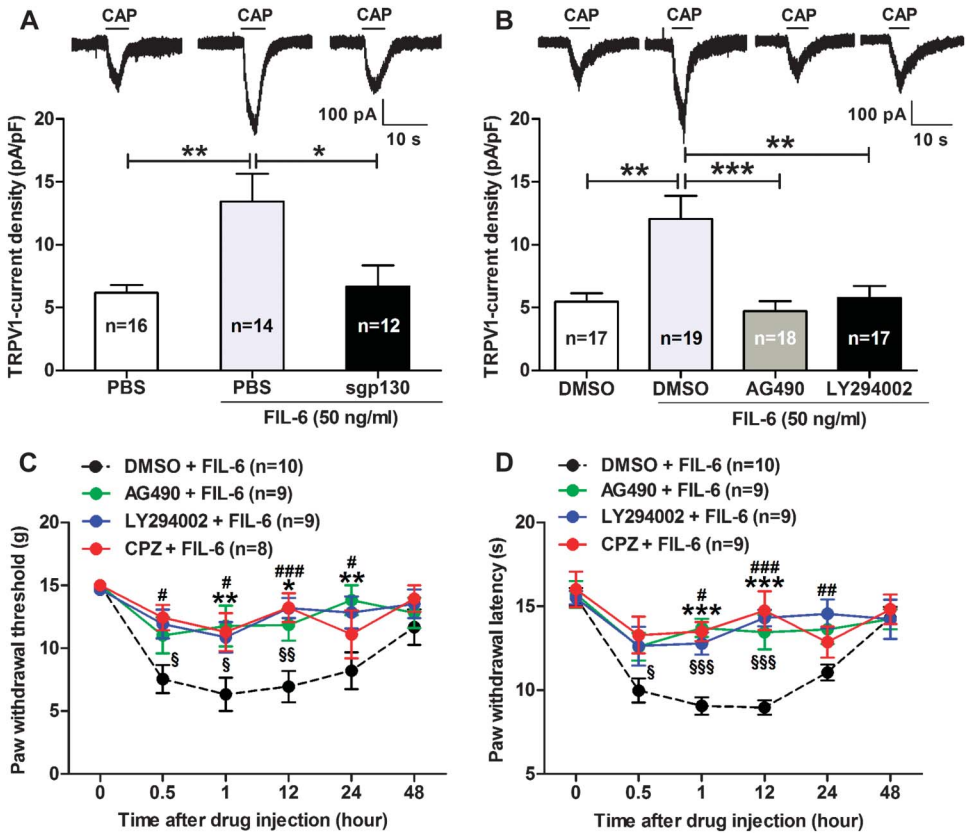

Figure 6. Activation of the JAK/PI3K signaling pathway is required for FIL-6-induced functional upregulation of TRPV1 in cultured dorsal root ganglion (DRG) neurons and pain hypersensitivity in normal rats. (A and B), Effects of IL-6/sIL-6R trans-signaling inhibitor sgp130 (A) as well as JAK inhibitor AG490 and PI3K inhibitor LY294002 (B) on FIL-6-induced potentiation of TRPV1 currents in cultured DRG neurons. Upper: representative traces of capsaicin (CAP, 0.5 μM for 3 seconds)-induced TRPV1 currents. Scale bar: 100 pA, 10 seconds; lower: summary of the TRPV1 current density (in pA/pF) in different groups. Note that after long-term (12 hours) exposure of cultured DRG neurons to FIL-6, the density of capsaicin-induced TRPV1 currents in the FIL-6 group is significantly increased as compared with the phosphate-buffered saline group, and this action of FIL-6-induced potentiation of TRPV1 currents is markedly blocked by sgp130, AG490, and LY294002, respectively. *$P < 0.05$, **$P < 0.01$, ***$P < 0.001$, 1-way analysis of variance, n = 12 to 19 per group. (C and D), Effects of intrathecal administration of JAK inhibitor AG490, PI3K inhibitor LY294002, or TRPV1 receptor antagonist capsazepine (CPZ) on FIL-6 induced mechanical allodynia (C) and thermal hyperalgesia (D) in normal rats. Note that all these inhibitors can significantly block the FIL-6-induced decreases in both paw withdrawal threshold and paw withdrawal latency in normal rats. *$P < 0.05$, **$P < 0.01$, ***$P < 0.001$ (the AG490 + FIL-6 group), *$P < 0.05$, **$P < 0.01$, ***$P < 0.001$ (the LY294002 + FIL-6 group), *$P < 0.05$, **$P < 0.01$, ***$P < 0.001$ (the CPZ + FIL-6 group), compared with the DMSO + FIL-6 group, 2-way analysis of variance, n = 8 to 10 per group.

(8.96 ± 0.43 seconds, n = 10) was also significantly restored by pretreatment with AG490 (13.46 ± 1.02 seconds, $P < 0.001$, n = 9), LY294002 (14.31 ± 0.49 seconds, $P < 0.001$, n = 9), or CPZ (14.74 ± 1.16 seconds, $P < 0.001$, n = 9) (2-way ANOVA, **Fig. 6D**). These results suggest that activation of the JAK/PI3K signaling pathway is required for both the FIL-6-induced functional upregulation of TRPV1 in DRG neurons and pain hypersensitivity in normal rats.

3.5. Functional upregulation of TRPV1 in dorsal root ganglion neurons contributes to the bone cancer–induced pain in MRMT-1 rats

To further determine whether the IL-6-induced functional upregulation of TRPV1 in DRG neurons through the activation of JAK/PI3K signaling pathway contributes to the pathogenesis of bone cancer pain, we first examined alterations of membrane TRPV1 expression and the capsaicin-induced TRPV1 currents in cancer rat DRG neurons. The results showed that the expression of membrane TRPV1 protein in ipsilateral L4 and L5 DRG was prominently increased on day 14 after surgery in MRMT-1 rats (1.37 ± 0.13) compared with sham rats (0.94 ± 0.02) ($P < 0.01$, 2-way ANOVA, n = 5, **Fig. 7A**). Accordingly, the density of capsaicin-induced TRPV1 currents in DRG neurons was also remarkably increased in MRMT-1 rats (63.94 ± 9.32 pA/pF, n = 17) compared with naive rats (39.92 ± 5.56 pA/pF, n = 18) and sham rats (37.93 ± 4.63 pA/pF, n = 20), respectively ($P < 0.05$, 1-way ANOVA, **Fig. 7B**). These data imply a functional upregulation of TRPV1 in DRG neurons in a rat model of bone cancer pain. Moreover, the behavioral study revealed that intrathecal administration of TRPV1 receptors antagonist CPZ (20 μg/10 μL) could apparently attenuate the bone cancer–induced mechanical allodynia and thermal hyperalgesia in MRMT-1 rats. For example, the bone cancer–induced decrease in PWT was significantly restored after the treatment with CPZ (10.51 ± 1.09*g* at day 18 and 9.07 ± 1.13*g* at day 19) compared with the vehicle PBS (4.14 ± 0.72*g* at day 18 and 3.76 ± 0.57*g* at day 19) ($P < 0.001$, 2-way ANOVA, n = 10/group, **Fig. 7C**). Similarly, the bone cancer–induced decrease in PWL was also markedly restored after the treatment with CPZ (13.25 ± 0.73 seconds at day 18 and 12.03 ± 0.92 seconds at day 19) compared with the vehicle PBS (8.82 ± 0.38 seconds at day 18 and 8.53 ± 0.60 seconds at day 19) ($P < 0.01$-0.001, 2-way ANOVA, n = 9 CPZ and 10 PBS, **Fig. 7D**). These results indicate that functional upregulation of TRPV1 in DRG neurons contributes to the bone cancer–induced pain in MRMT-1 rats.

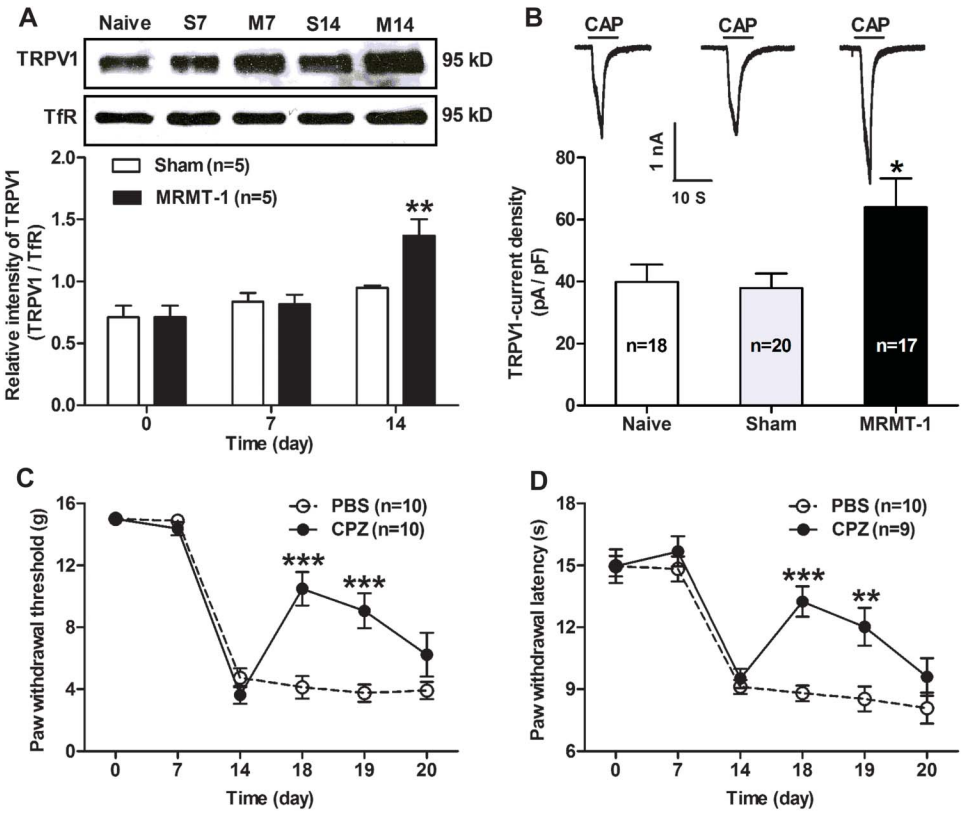

Figure 7. Functional upregulation of TRPV1 in dorsal root ganglion (DRG) neurons contributes to the bone cancer–induced pain in mammary rat metastasis tumor (MRMT-1) rats. (A), Western blot of membrane TRPV1 protein expression in the DRG of MRMT-1 rats. Upper: representative of Western blot bands; lower: analysis of the relative intensity of TRPV1 membrane protein. TfR (transferrin receptor) is used as an internal control. Note that the expression of membrane TRPV1 protein in ipsilateral L4 and L5 DRG is statistically increased on day 14 after surgery in MRMT-1 rats compared with sham rats. $^{**}P < 0.01$, 2-way analysis of variance (ANOVA), n = 5 per group. (B), Whole-cell patch-clamp recording of capsaicin-induced TRPV1 currents in DRG neurons. Upper: representative traces of capsaicin (CAP, 0.5 μM for 3 seconds)-induced TRPV1 currents. Scale bar: 100 pA, 10 seconds; lower: summary of the TRPV1 current density (in pA/pF) in DRG neurons of naive, sham, and MRMT-1 rats. Note that the density of capsaicin-induced TRPV1 currents in DRG neurons is prominently increased in MRMT-1 rats compared with naive and sham rats, $^{*}P < 0.05$, 1-way ANOVA, n = 18 (naive), 20 (sham), and 17 (MRMT-1). (C and D), Effects of TRPV1 receptor antagonist CPZ on the bone cancer–induced mechanical allodynia and thermal hyperalgesia in MRMT-1 rats. Note that intrathecal administration of CPZ (20 μg/10 μL) can significantly restore the bone cancer–induced decreases in paw withdrawal threshold (C) and paw withdrawal latency (D) in MRMT-1 rats. $^{**}P < 0.01$, $^{***}P < 0.001$, 2-way ANOVA, n = 9 to 10 per group. M, MRMT-1; S, sham.

3.6. Suppression of functional upregulation of TRPV1 in dorsal root ganglion neurons by the inhibition of JAK/PI3K signaling pathway reduces the overexcitability of dorsal root ganglion neurons and pain hypersensitivity in bone cancer rats

Then, we explored whether suppression of functional upregulation of TRPV1 in DRG neurons by the inhibition of JAK/PI3K signaling pathway could reduce the hyperexcitability of DRG neurons and pain hypersensitivity in bone cancer rats. We examined the effects of pretreatment or posttreatment with JAK/PI3K inhibitor on functional expression of TRPV1 in DRG neurons as well as on DRG neuron excitability and pain behaviors in bone cancer rats. In the pretreatment experiments, we found that pretreatment with IL-6/sIL-6R trans-signaling inhibitor sgp130, JAK inhibitor AG490, or PI3K inhibitor LY294002 could apparently block the bone cancer–induced functional upregulation of TRPV1 in DRG neurons of MRMT-1 rats (**Figs. 8A to D**). The relative intensity of TRPV1 membrane protein in ipsilateral L4 and L5 DRG of bone cancer rats was statistically decreased in the sgp130 group (0.88 ± 0.09 sgp130 vs 1.23 ± 0.04 PBS, $P < 0.01$), the AG490 group (0.81 ± 0.08, $P < 0.01$), and the LY294002 group (0.95 ± 0.06, $P < 0.05$), as compared with the vehicle group (DMSO 1.18 ± 0.08) (1-way ANOVA, n = 5, **Figs. 8A-B**). Moreover, the density of capsaicin-induced TRPV1 currents (in pA/pF) in cancer rat DRG neurons also was remarkably reduced in the sgp130 group (29.72 ± 4.95 sgp130 vs 71.99 ± 14.01 PBS, $P < 0.01$, n = 25 sgp130 and 21 PBS), the AG490 group (19.83 ± 4.50, $P < 0.001$, n = 21), and the LY294002 group (24.72 ± 3.59, $P < 0.01$, n = 22), as compared with the vehicle group (DMSO 80.63 ± 14.56, n = 24) (1-way ANOVA, **Figs. 8C-D**). Accordingly, both the bone cancer–induced hyperexcitability of DRG neurons and pain hypersensitivity were also dramatically reduced by pretreatment with either JAK inhibitor AG490 or PI3K inhibitor LY294002 (**Figs. 8E to H**). For example, the spike numbers of APs evoked by a 500-millisecond 300 pA depolarizing current pulse in cancer rat DRG neurons were markedly decreased in the AG490 group (3.65 ± 1.18, $P < 0.05$, n = 23) and the LY294002 group (2.71 ± 1.29, $P < 0.01$, n = 21) as compared with the vehicle DMSO group (8.63 ± 1.66, n = 19) (1-way ANOVA, **Figs. 8E-F**). Additionally, both the bone cancer–induced decreases in PWT and PWL were significantly blocked either by pretreatment with AG490 (PWT: 11.88 ± 1.25*g* and PWL: 13.62 ± 1.28 seconds, n = 8) or by LY294002 (PWT: 11.07 ± 1.52*g* and PWL: 11.98 ± 0.99 seconds, n = 7) in contrast to vehicle DMSO (PWT: 5.72 ± 1.04*g* and PWL: 8.36 ± 0.45 s, n = 7) ($P < 0.05$-0.01, 1-way ANOVA, **Figs. 8G-H**).

Similarly, in the posttreatment experiments, we found that the bone cancer–induced functional upregulation of TRPV1 in DRG neurons could also be blocked by posttreatment with IL-6/sIL-6R trans-signaling inhibitor sgp130, JAK inhibitor AG490, or PI3K inhibitor LY294002 (**Figs. 9A to D**). The relative intensity of TRPV1 membrane protein in ipsilateral L4 and L5 DRG of bone cancer rats was statistically decreased in the sgp130 group (0.84 ± 0.09 sgp130 vs 1.21 ± 0.01 PBS, $P < 0.05$), the AG490 group (0.99 ± 0.06, $P < 0.05$), and the LY294002 group (0.85 ± 0.05, $P < 0.01$), as compared with the vehicle group (DMSO 1.25 ± 0.09) (1-way ANOVA, n = 4, **Figs. 9A-B**). The density of capsaicin-induced TRPV1 currents (in pA/pF) in cancer rat DRG neurons was also prominently reduced in the sgp130 group (24.57 ± 5.37 sgp130 vs 70.24 ± 12.01 PBS, $P < 0.001$, n = 24), the AG490 group (25.57 ± 5.02, $P < 0.001$, n = 25), and the LY294002 group (32.98 ± 4.71, $P < 0.01$, n = 30), as compared with the vehicle group (DMSO 77.04 ± 13.02, n = 25) (1-way ANOVA, **Figs. 9C-D**). As expected, both the bone cancer–induced hyperexcitability of DRG neurons and pain hypersensitivity were also markedly attenuated by posttreatment with either JAK inhibitor AG490 or PI3K inhibitor LY294002 (**Figs. 9E to H**). The spike numbers of APs evoked by a 500-millisecond 300 pA depolarizing current pulse in cancer rat DRG neurons were decreased in the AG490 group (3.64 ± 1.05, $P < 0.05$, n = 25) and the LY294002 group (3.96 ± 1.26, $P < 0.05$, n = 24) as compared with the vehicle DMSO group (8.78 ± 1.72, n = 23) (1-way ANOVA, **Figs. 9E-F**). With regard to pain behaviors, both the bone cancer–induced decreases in PWT and PWL were significantly restored either by posttreatment with AG490 (PWT: 12.87 ± 0.95*g* and PWL: 12.05 ± 0.94 seconds, n = 9) or by LY294002 (PWT: 11.42 ± 1.29*g* and PWL: 13.26 ± 1.27 seconds, n = 8) as compared with vehicle DMSO (PWT: 5.87 ± 1.23*g* and PWL: 8.37 ± 0.74 seconds, n = 7) ($P < 0.05$-0.001, 1-way ANOVA, **Figs. 9G-H**).

Taken together, these results suggest that suppression of functional upregulation of TRPV1 in DRG neurons by the inhibition of JAK/PI3K signaling pathway, either before surgery or after surgery, can reduce the hyperexcitability of DRG neurons and pain hypersensitivity in bone cancer rats. Therefore, IL-6 may play a role in bone cancer–induced pain by upregulating TRPV1 channels in DRG neurons through JAK/PI3K signaling pathway.

4. Discussion

We here provide multiple lines of evidence showing that IL-6 plays a vital role in sensitization of DRG neurons and bone cancer pain development through IL-6/sIL-6R trans-signaling. First, we found an elevated expression of IL-6 in cancer rat DRG, which was temporally correlated with the emergence of pain hyperalgesia.[81] Moreover, we suggest that IL-6 contributes to the pathogenesis of bone cancer pain through trans-signaling because only sIL-6R was detected in the DRG. Meanwhile, we discovered an increased expression of sIL-6R and gp130 in cancer rat DRG, which was consistent with IL-6's alterations. Second, we demonstrated that extraneous application of FIL-6, an IL-6/sIL-6R complex that has been widely used in previous studies,[31,32,67] could induce overexcitability of DRG neurons and pain hypersensitivity in normal rats. In support of our notion that IL-6 exerts its roles in DRG neurons through IL-6/IL-6R trans-signaling, we indeed found that all of these actions of FIL-6 could be blocked by sgp130, an inhibitor of IL-6/sIL-6R trans-signaling pathway.[10,12,32,65] Similarly, in a rat cancer model, we further clarified that the inhibition of IL-6/sIL-6R trans-signaling by sgp130 could reduce bone cancer–induced hyperexcitability of DRG neurons and pain hypersensitivity. We thus suggest that enhanced IL-6 contributes to the sensitization of DRG neurons and bone cancer pain development through IL-6/sIL-6R trans-signaling. Of course, IL-6 can also enhance cancer pain through spinal cord mechanisms especially after intrathecal injection. It has been found that spinal administration of IL-6 induces central sensitization and heat hyperalgesia in rats, which is suggested to occur through regulating synaptic and neuronal activity in the superficial spinal cord.[36] A recent study has shown that spinal IL-6 also contributes to central sensitization and arthritic pain.[73] Interleukin-6 can induce spinal glial activation, thus playing an important role in neuropathic pain after peripheral nerve injury.[3,18,40] An increased expression of spinal IL-6 in cancer rats suggests a central role of IL-6 in bone cancer–induced pain.[19,48]

Furthermore, we provide novel evidence validating that IL-6 plays a role in bone cancer pain by upregulating TRPV1 channels in DRG

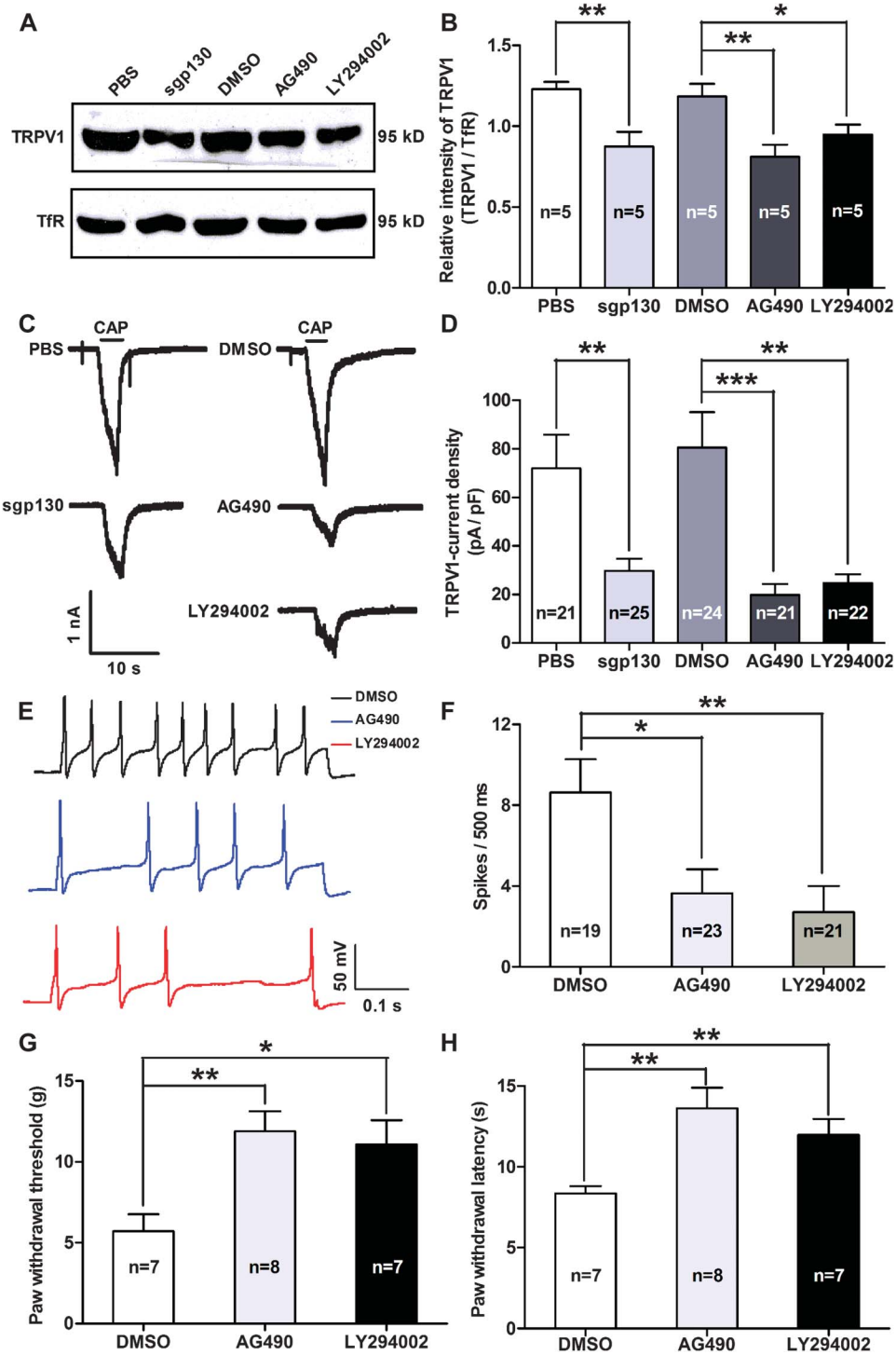

Figure 8. Pretreatment with IL-6/sIL-6 trans-signaling inhibitor sgp130, JAK inhibitor AG490, or PI3K inhibitor LY294002 reduces the functional upregulation of TRPV1 in dorsal root ganglion (DRG) neurons, represses the neuronal hyperexcitability, and prevents the bone cancer–induced pain in mammary rat metastasis tumor (MRMT-1) rats. (A and B), Western blot of membrane TRPV1 protein expression. (A), Representative of Western blot bands. (B), Analysis of the relative intensity of TRPV1 membrane protein. TfR (transferrin receptor) is used as an internal control. Note that all these inhibitors can significantly reduce the bone cancer–induced increase of membrane TRPV1 protein expression in ipsilateral L4 and L5 DRG of MRMT-1 rats. $^{*}P < 0.05$, $^{**}P < 0.01$, 1-way analysis of variance (ANOVA), n = 5 per group. (C and D), Whole-cell patch-clamp recording of capsaicin-induced TRPV1 currents on acutely dissociated DRG neurons of MRMT-1 rats. (C), Representative traces of capsaicin (CAP, 0.5 μM for 3 seconds)-induced TRPV1 currents. Scale bar: 1 nA, 10 seconds. (D), Summary of the TRPV1 current density (in pA/pF) in DRG neurons in rats pretreated with sgp130, AG490, LY294002 as well as the vehicle phosphate-buffered saline and DMSO, respectively. Note that all these inhibitors can dramatically block the bone cancer–induced potentiation of TRPV1 currents in DRG neurons. $^{**}P < 0.01$, $^{***}P < 0.001$, 1-way ANOVA, n = 21 to 25 per group. (E and F), Effects of AG490 and LY294002 on DRG neuron excitability of MRMT-1 rats. (E), Representative traces of action potential (AP) discharges evoked by a 500-millisecond 300 pA depolarizing current pulse. Scale bar: 50 mV, 0.1 seconds. (F), Summary of AP numbers in DRG neurons in rats pretreated with AG490, LY294002, and the vehicle DMSO, respectively. Note that both AG490 and LY294002 can prominently block the bone cancer–induced increase in AP numbers of DRG neurons. $^{*}P < 0.05$, $^{**}P < 0.01$, 1-way ANOVA, n = 19 (DMSO), 23 (AG490), and 21 (LY294002). (G and H), Effects of pretreatment with AG490 or LY294002 on the mechanical allodynia and thermal hyperalgesia of bone cancer rats. Note that both AG490 and LY294002 can remarkably prevent the bone cancer–induced decreases in paw withdrawal threshold and paw withdrawal latency in MRMT-1 rats. $^{*}P < 0.05$, $^{**}P < 0.01$, 1-way ANOVA, n = 7 (DMSO), 8 (AG490), and 7 (LY294002).

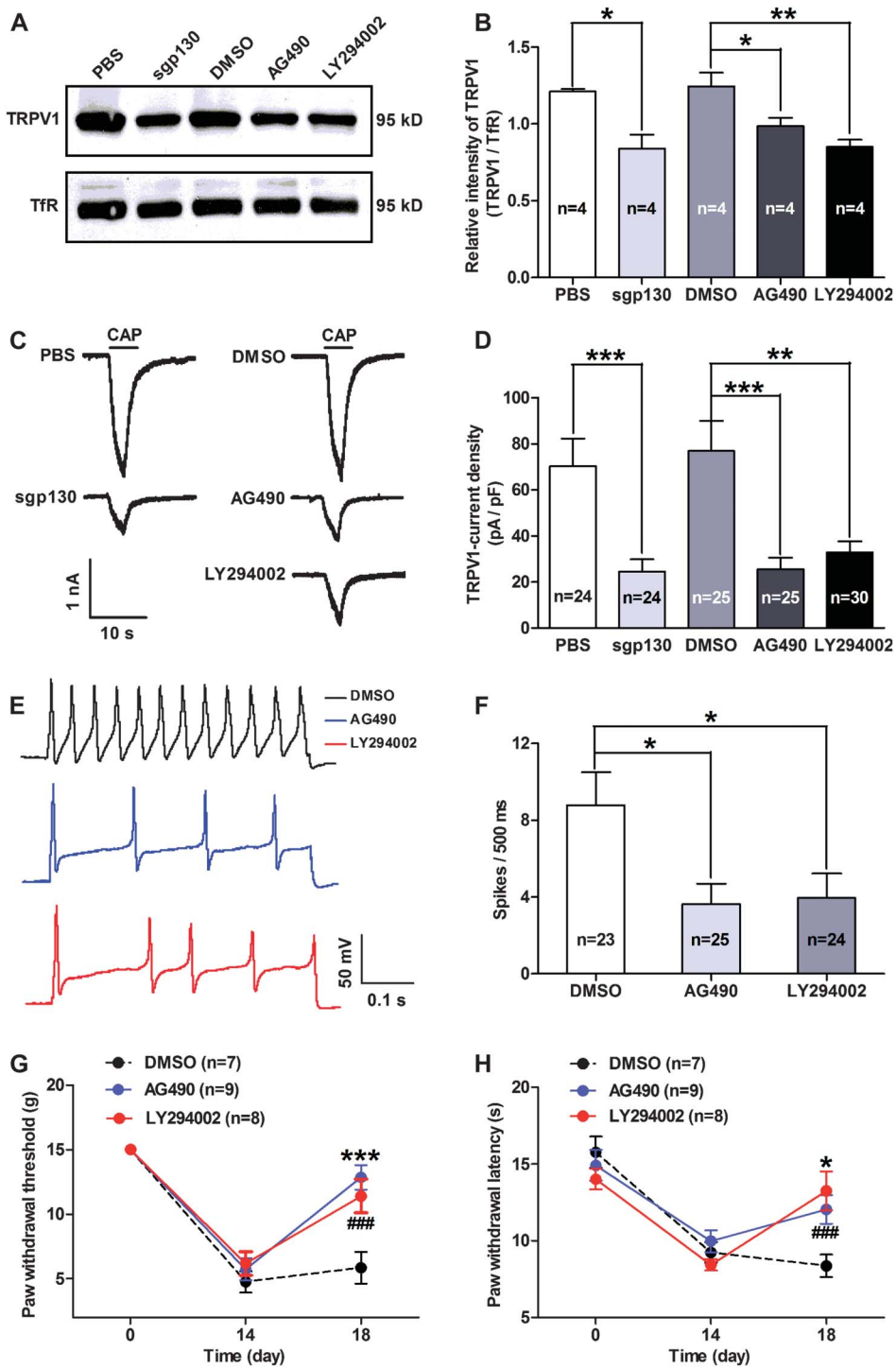

Figure 9. Posttreatment with IL-6/sIL-6 trans-signaling inhibitor sgp130, JAK inhibitor AG490, or PI3K inhibitor LY294002 blocks the functional upregulation of TRPV1 in dorsal root ganglion (DRG) neurons, suppresses the neuronal hyperexcitability, and attenuates the bone cancer–induced pain in mammary rat metastasis tumor (MRMT-1) rats. (A and B), Western blot of membrane TRPV1 protein expression. (A), Representative of Western blot bands. (B), Analysis of the relative intensity of TRPV1 membrane protein. TfR (transferrin receptor) is used as an internal control. Note that all these inhibitors can significantly block the bone cancer–induced increase of membrane TRPV1 protein expression in ipsilateral L4 and L5 DRG of MRMT-1 rats. $^{*}P < 0.05$, $^{**}P < 0.01$, 1-way analysis of variance (ANOVA), n = 4 per group. (C and D), Whole-cell patch-clamp recording of capsaicin-induced TRPV1 currents on acutely dissociated DRG neurons of MRMT-1 rats. (C), Representative traces of capsaicin (CAP, 0.5 μM for 3 seconds)-induced TRPV1 currents. Scale bar: 1 nA, 10 seconds. (D), Summary of the TRPV1 current density in DRG neurons in rats posttreated with sgp130, AG490, LY294002 as well as the vehicle phosphate-buffered saline and DMSO, respectively. Note that all these inhibitors can dramatically reduce the bone cancer–induced potentiation of TRPV1 currents in DRG neurons. $^{**}P < 0.01$, $^{***}P < 0.001$, 1-way ANOVA, n = 24 to 30 per group. (E and F), Effects of AG490 and LY294002 on DRG neuron excitability of MRMT-1 rats. (E), Representative traces of action potential (AP) discharges evoked by a 500-millisecond 300 pA depolarizing current pulse. Scale bar: 50 mV, 0.1 seconds. (F), Summary of AP numbers in DRG neurons in rats posttreated with AG490, LY294002, and the vehicle DMSO, respectively. Note that both AG490 and LY294002 can prominently block the bone cancer–induced increase of AP numbers in DRG neurons. $^{*}P < 0.05$, 1-way ANOVA, n = 23 (DMSO), 25 (AG490), and 24 (LY294002). (G and H), Effects of posttreatment with AG490 or LY294002 on the mechanical allodynia and thermal hyperalgesia of bone cancer rats. Note that both AG490 and LY294002 can remarkably restore the bone cancer–induced decreases in paw withdrawal threshold and paw withdrawal latency in MRMT-1 rats. $^{*}P < 0.05$, $^{***}P < 0.001$ (AG490), $^{***}P < 0.001$ (LY294002), compared with DMSO, 1-way ANOVA, n = 7 (DMSO), 9 (AG490), and 8 (LY294002).

neurons through the activation of JAK/PI3K signaling pathway. We found that expression of TRPV1 protein but not mRNA was significantly increased even after long-term exposure of DRG neurons to FIL-6, suggesting a possible translational modulation.[62] The translational regulation of TRPV1 has been shown in the DRG after inflammation or nerve growth factor (NGF) treatment,[28] or by tumor necrosis factor α (TNF-α) stimulation,[15] while the NGF-induced rapid membrane insertion of TRPV1 also has been found in cultured DRG neurons.[80] Recently, Melemedjian et al.[50] have revealed a potential role of activity-dependent translation control of IL-6 in primary afferent nociceptive plasticity; thus, the IL-6-induced mechanical allodynia is attenuated by inhibitors of translation but not transcription. We observed that protein synthesis inhibitor anisomycin blocked FIL-6-induced increases both in total and membrane TRPV1 protein after a long-term but not a short-term exposure of DRG neurons to FIL-6. This implies that IL-6 induces a rapid upregulation of TRPV1 in the early phase through a directed TRPV1 trafficking to the surface membrane, while in the late phase, a sustained increase in TRPV1 protein is likely dependent on nascent protein synthesis through translational regulation. In agreement with previous studies,[15,28] we did not detect any change in TRPV1 mRNA levels in the DRG either after short-term or after long-term FIL-6 treatment, further supporting our notion that the IL-6-induced upregulation of TRPV1 is a transcription-independent regulation. Along with an elevated expression of membrane TRPV1 protein, we discovered that the capsaicin-induced TRPV1 currents were potentiated after long-term FIL-6 treatment, implying that the FIL-6-induced increase of membrane TRPV1 on the DRG neurons is functional. Indeed, IL-6/gp130 complex is involved in heat hypersensitivity by increasing TRPV1 currents.[2,58] Therefore, blockade of TRPV1 receptor using a selective antagonist capsazepine or a null mutation of TRPV1 gene[2,38] can rescue FIL-6-induced pain hypersensitivity.

Multiple signaling pathways including JAK/STAT, MAPK/ERK, and PI3K/AKT pathways are involved in IL-6-mediated physiological and pathophysiological functions.[20,21,27,69] We found that JAK inhibitor AG490 could block FIL-6-induced upregulation of total and membrane TRPV1 protein, suggesting that JAK is involved in IL-6-mediated TRPV1 regulation at a translational level. Moreover, IL-6-induced PI3K activation can be shown by AKT phosphorylation both after short-term and long-term exposure of DRG neurons to FIL-6. In addition, the JAK inhibitor AG490 can also block FIL-6-induced phosphorylation of AKT, a downstream effector molecule of PI3K. These results suggest that JAK may upregulate TRPV1 protein at a translational level through PI3K/AKT pathway in FIL-6-treated DRG neurons. In support of this notion, we discovered that both FIL-6-induced functional upregulation of TRPV1 and pain hypersensitivity could be blocked by JAK inhibitor AG490 or PI3K inhibitor LY294002. Certainly, the ERK pathway is also involved in IL-6-mediated protein translation in sensory neurons,[50] and activation of PI3K by NGF can promote TRPV1 trafficking to the plasma membrane.[70] However, PI3K can activate ERK in DRG neurons and mediate inflammatory heat hyperalgesia through TRPV1 sensitization.[83] Hence, we cannot exclude the contribution of the ERK pathway, either directly activated by IL-6 or indirectly activated by PI3K, to FIL-6-induced functional upregulation of TRPV1 in DRG neurons. Indeed, we found that the MEK inhibitor PD98059 blocked FIL-6-induced upregulation of TRPV1 protein in DRG neurons.

Compared with delayed upregulation of TRPV1 after IL-6 treatment, TNF-α has been shown to cause a rapid upregulation of TRPV1 in DRG neurons within 1 h.[15] Tumor necrosis factor α induces fast sensitization and upregulation of TRPV1 through p38/MAP kinase– and protein kinase C (PKC)-dependent pathways, thereby playing a role in heat hyperalgesia in a mouse cancer model.[15] Although TNF-α can induce upregulation of

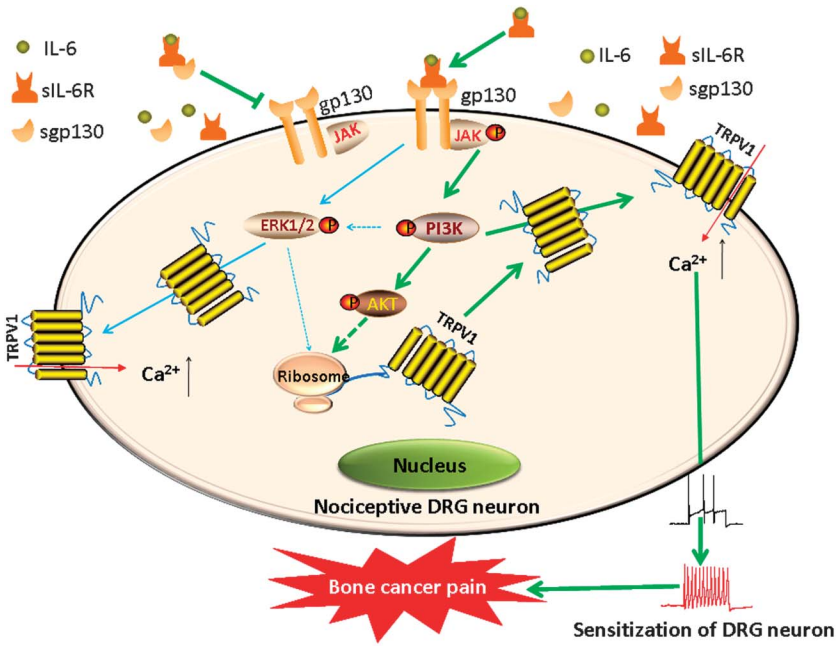

Figure 10. Possible molecular mechanisms underlying the interleukin-6 (IL-6)-mediated sensitization of dorsal root ganglion (DRG) neurons and the development of bone cancer pain through IL-6/sIL-6R trans-signaling. The expression of IL-6 and its soluble receptor sIL-6R is significantly increased in cancer rat DRG neurons. The elevated IL-6 binds to sIL-6R and induces homodimerization of gp130, which subsequently activates the JAK/PI3K/AKT signaling cascade and then triggers the functional upregulation of TRPV1 in DRG neurons. The potentiated TRPV1 leads to an increase in calcium influx and then results in the sensitization of DRG neurons and the pathogenesis of bone cancer pain. Moreover, the ERK pathway, either directly activated by IL-6 or indirectly activated by PI3K, is also involved in IL-6-induced functional upregulation of TRPV1 in DRG neurons.

TRPV1 within several hours,[37,55] this upregulation is dependent on ERK but not p38/MAP kinase.[26,66] Thus, IL-6 may upregulate TRPV1 through intracellular pathways that are different from those of TNF-α.

It is well established that functional upregulation of TRPV1 in DRG neurons plays a critical role in bone cancer pain.[23,24,35,57,60,77] Indeed, we found that both the membrane TRPV1 expression and the capsaicin-induced TRPV1 currents are significantly increased in cancer rat DRG neurons, and intrathecal administration of TRPV1 antagonist capsazepine attenuates bone cancer–induced pain. It has been shown that the activation of TRPV1 may induce an increase in intracellular calcium level.[4,14,39] The rise in calcium leads to the activation of multiple intracellular calcium–sensitive protein kinases, which are responsible for the modulation of sensory neurons excitability.[6,39,43,54] Together with our current findings that sgp130 not only represses the functional upregulation of TRPV1 in DRG neurons but also reduces the neuronal hyperexcitability and attenuates pain hypersensitivity in bone cancer rats, we suggest that IL-6 may play its role in bone cancer–induced pain by promoting functional upregulation of TRPV1 in DRG neurons through IL-6/sIL-6R trans-signaling. Additionally, our in vivo study further proved that suppression of functional upregulation of TRPV1 in DRG neurons through the inhibition of JAK/PI3K signaling pathway, either before surgery or after surgery, could reduce the hyperexcitability of DRG neurons and pain hypersensitivity in bone cancer rats. Thus, activation of the JAK/PI3K signaling cascade is involved in IL-6-induced functional upregulation of TRPV1 in DRG neurons, which subsequently leads to the sensitization of primary sensory neurons and bone cancer pain development.

Aside from intrathecal administration, we found that all inhibitors used for these signaling pathways (IL-6/JAK/PI3K/TRPV1) could also prevent IL-6- and bone cancer–induced pain hypersensitivity after being intraplantarly delivered to rats (supplementary data, Figs. S2 and S3 available online as Supplemental Digital Content at http://links.lww.com/PAIN/A63 and http://links.lww.com/PAIN/A64). We conclude that a role for these pathways in bone cancer–induced hyperalgesia also exists at the peripheral terminals of DRG neurons.

Certainly, we cannot rule out the role of sodium channels in the actions of IL-6 because of the fact that IL-6 can increase the neuronal spike number, which is related to the modulation of sodium channels.[11,49,75] In fact, Yan et al.[79] have reported that IL-6 enhances the excitability of dural afferents through the modulation of Nav1.7 sodium channels. Activation of peripheral TRPV1 receptors in the colon leads to a functional upregulation of sodium channels in bladder sensory neurons,[41] while axon reflexes evoked by TRPV1 activation are mediated by tetrodotoxin-resistant sodium channels in intestinal afferent nerves.[51] Thus, IL-6 may also sensitize DRG neurons through the modulation of sodium channels, either in a direct manner or through TRPV1 activation. Besides IL-6, other proinflammatory cytokines including IL-1β[5] and TNF-α[30] can also increase the activities of tetrodotoxin-resistant sodium channels or promote their expression in uninjured DRG neurons after nerve injury.[25] Whether these cytokines have a synergistic effect with regard to the ability of IL-6 to sensitize DRG neurons and mediate bone cancer pain needs be further explored.

In conclusion, our data suggest that IL-6 plays a crucial role in the sensitization of DRG neurons and bone cancer pain development through IL-6/sIL-6R trans-signaling. Moreover, functional upregulation of TRPV1 in DRG neurons through the activation of JAK/PI3K signaling pathway contributes to the effects of IL-6 on the pathogenesis of bone cancer pain. We here disclose a novel intracellular pathway, the IL-6/JAK/PI3K/TRPV1 signaling cascade (**Fig.10**), which may underlie the development of peripheral sensitization and bone cancer–induced pain.

Conflict of interest statement

The authors have no conflicts of interest to declare.

The present work was supported by grants from the National Natural Science Foundation of China (81371237, 31171063), the Beijing Natural Science Foundation (7112079), the special foundation for public welfare profession scientific research program from the Ministry of Health of the People's Republic of China (201302013-01), and the "973" Program of the Ministry of Science and Technology of China (2013CB531905).

Acknowledgements

The authors thank Hong-Yan Zhao and Hong Jiang at the Neuroscience Research Institute and Department of Neurobiology, Peking University, for their contributions to part of the behavioral test in the revised article.

Author contributions: D. Fang, L.-Y. Kong, and J. Cai contributed equally to this work. D. Fang conducted the Western blot and the electrophysiological studies, participated in the design of the study, and drafted the article. L.-Y. Kong and J. Cai participated in the behavioral test and performed the statistical analysis. S. Li and X.-D. Liu participated in the PCR assay, Western blot, and part of the behavioral test. J.-S. Han participated in part of the design of the study. G.-G. Xing conceived of the study, participated in its design and coordination, and drafted the article. All authors have read and approved the final article.

Appendix A. Supplemental Digital Content

Supplemental Digital Content associated with this article can be found online at http://links.lww.com/PAIN/A62, http://links.lww.com/PAIN/A63, http://links.lww.com/PAIN/A64, http://links.lww.com/PAIN/A65.

Article history:
Received 7 January 2015
Received in revised form 1 March 2015
Accepted 3 March 2015
Available online 10 March 2015

References

[1] Abdel Meguid MH, Hamad YH, Swilam RS, Barakat MS. Relation of interleukin-6 in rheumatoid arthritis patients to systemic bone loss and structural bone damage. Rheumatol Int 2013;33:697–703.
[2] Andratsch M, Mair N, Constantin CE, Scherbakov N, Benetti C, Quarta S, Vogl C, Sailer CA, Uceyler N, Brockhaus J, Martini R, Sommer C, Zeilhofer HU, Muller W, Kuner R, Davis JB, Rose-John S, Kress M. A key role for gp130 expressed on peripheral sensory nerves in pathological pain. J Neurosci 2009; 29:13473–83.
[3] Arruda JL, Sweitzer S, Rutkowski MD, DeLeo JA. Intrathecal anti-IL-6 antibody and IgG attenuates peripheral nerve injury-induced mechanical allodynia in the rat: possible immune modulation in neuropathic pain. Brain Res 2000;879:216–25.
[4] Bevan S, Quallo T, Andersson DA. TRPV1. Handb Exp Pharmacol 2014; 222:207–45.
[5] Binshtok AM, Wang H, Zimmermann K, Amaya F, Vardeh D, Shi L, Brenner GJ, Ji RR, Bean BP, Woolf CJ, Samad TA. Nociceptors are interleukin-1beta sensors. J Neurosci 2008;28:14062–73.
[6] Boillat A, Alijevic O, Kellenberger S. Calcium entry via TRPV1 but not ASICs induces neuropeptide release from sensory neurons. Mol Cell Neurosci 2014;61:13–22.

[7] Brenn D, Richter F, Schaible HG. Sensitization of unmyelinated sensory fibers of the joint nerve to mechanical stimuli by interleukin-6 in the rat: an inflammatory mechanism of joint pain. Arthritis Rheum 2007;56:351–9.
[8] Brito R, Sheth S, Mukherjea D, Rybak LP, Ramkumar V. TRPV1: a potential drug target for treating various diseases. Cells 2014;3:517–45.
[9] Busch-Dienstfertig M, Gonzalez-Rodriguez S. IL-4, JAK-STAT signaling, and pain. JAKSTAT 2013;2:e27638.
[10] Campbell IL, Erta M, Lim SL, Frausto R, May U, Rose-John S, Scheller J, Hidalgo J. Trans-signaling is a dominant mechanism for the pathogenic actions of interleukin-6 in the brain. J Neurosci 2014;34:2503–13.
[11] Chahine M, O'Leary ME. Regulation/modulation of sensory neuron sodium channels. Handb Exp Pharmacol 2014;221:111–35.
[12] Chalaris A, Garbers C, Rabe B, Rose-John S, Scheller J. The soluble interleukin 6 receptor: generation and role in inflammation and cancer. Eur J Cell Biol 2011;90:484–94.
[13] Chaplan SR, Bach FW, Pogrel JW, Chung JM, Yaksh TL. Quantitative assessment of tactile allodynia in the rat paw. J Neurosci Methods 1994; 53:55–63.
[14] Chung MK, Guler AD, Caterina MJ. TRPV1 shows dynamic ionic selectivity during agonist stimulation. Nat Neurosci 2008;11:555–64.
[15] Constantin CE, Mair N, Sailer CA, Andratsch M, Xu ZZ, Blumer MJ, Scherbakov N, Davis JB, Bluethmann H, Ji RR, Kress M. Endogenous tumor necrosis factor alpha (TNFalpha) requires TNF receptor type 2 to generate heat hyperalgesia in a mouse cancer model. J Neurosci 2008; 28:5072–81.
[16] Ding X, Cai J, Li S, Liu XD, Wan Y, Xing GG. BDNF contributes to the development of neuropathic pain by induction of spinal long-term potentiation via SHP2 associated GluN2B-containing NMDA receptors activation in rats with spinal nerve ligation. Neurobiol Dis 2014;73C:428–51.
[17] Dixon WJ. Efficient analysis of experimental observations. Annu Rev Pharmacol Toxicol 1980;20:441–62.
[18] Dominguez E, Rivat C, Pommier B, Mauborgne A, Pohl M. JAK/STAT3 pathway is activated in spinal cord microglia after peripheral nerve injury and contributes to neuropathic pain development in rat. J Neurochem 2008;107:50–60.
[19] Dong Y, Mao-Ying QL, Chen JW, Yang CJ, Wang YQ, Tan ZM. Involvement of EphB1 receptor/ephrinB1 ligand in bone cancer pain. Neurosci Lett 2011;496:163–7.
[20] Eulenfeld R, Dittrich A, Khouri C, Muller PJ, Mutze B, Wolf A, Schaper F. Interleukin-6 signalling: more than Jaks and STATs. Eur J Cell Biol 2012; 91:486–95.
[21] Fang XX, Jiang XL, Han XH, Peng YP, Qiu YH. Neuroprotection of interleukin-6 against NMDA-induced neurotoxicity is mediated by JAK/ STAT3, MAPK/ERK, and PI3K/AKT signaling pathways. Cell Mol Neurobiol 2013;33:241–51.
[22] Geng SJ, Liao FF, Dang WH, Ding X, Liu XD, Cai J, Han JS, Wan Y, Xing GG. Contribution of the spinal cord BDNF to the development of neuropathic pain by activation of the NR2B-containing NMDA receptors in rats with spinal nerve ligation. Exp Neurol 2010;222:256–66.
[23] Ghilardi JR, Rohrich H, Lindsay TH, Sevcik MA, Schwei MJ, Kubota K, Halvorson KG, Poblete J, Chaplan SR, Dubin AE, Carruthers NI, Swanson D, Kuskowski M, Flores CM, Julius D, Mantyh PW. Selective blockade of the capsaicin receptor TRPV1 attenuates bone cancer pain. J Neurosci 2005; 25:3126–31.
[24] Han Y, Li Y, Xiao X, Liu J, Meng XL, Liu FY, Xing GG, Wan Y. Formaldehyde up-regulates TRPV1 through MAPK and PI3K signaling pathways in a rat model of bone cancer pain. Neurosci Bull 2012;28:165–72.
[25] He XH, Zang Y, Chen X, Pang RP, Xu JT, Zhou X, Wei XH, Li YY, Xin WJ, Qin ZH, Liu XG. TNF-alpha contributes to up-regulation of Nav1.3 and Nav1.8 in DRG neurons following motor fiber injury. PAIN 2010;151:266–79.
[26] Hensellek S, Brell P, Schaible HG, Brauer R, Segond von BG. The cytokine TNFalpha increases the proportion of DRG neurones expressing the TRPV1 receptor via the TNFR1 receptor and ERK activation. Mol Cell Neurosci 2007;36:381–91.
[27] Jazayeri JA, Upadhyay A, Vernallis AB, Carroll GJ. Targeting the glycoprotein 130 receptor subunit to control pain and inflammation. J Interferon Cytokine Res 2010;30:865–73.
[28] Ji RR, Samad TA, Jin SX, Schmoll R, Woolf CJ. p38 MAPK activation by NGF in primary sensory neurons after inflammation increases TRPV1 levels and maintains heat hyperalgesia. Neuron 2002;36:57–68.
[29] Jiang H, Fang D, Kong LY, Jin ZR, Cai J, Kang XJ, Wan Y, Xing GG. Sensitization of neurons in the central nucleus of the amygdala via the decreased GABAergic inhibition contributes to the development of neuropathic pain-related anxiety-like behaviors in rats. Mol Brain 2014;7: 72–93.
[30] Jin X, Gereau RW. Acute p38-mediated modulation of tetrodotoxin-resistant sodium channels in mouse sensory neurons by tumor necrosis factor-alpha. J Neurosci 2006;26:246–55.
[31] Jostock T, Blinn G, Renne C, Kallen KJ, Rose-John S, Mullberg J. Immunoadhesins of interleukin-6 and the IL-6/soluble IL-6R fusion protein hyper-IL-6. J Immunol Methods 1999;223:171–83.
[32] Jostock T, Mullberg J, Ozbek S, Atreya R, Blinn G, Voltz N, Fischer M, Neurath MF, Rose-John S. Soluble gp130 is the natural inhibitor of soluble interleukin-6 receptor transsignaling responses. Eur J Biochem 2001;268:160–7.
[33] Julius D. TRP channels and pain. Annu Rev Cell Dev Biol 2013;29: 355–84.
[34] Kao DJ, Li AH, Chen JC, Luo RS, Chen YL, Lu JC, Wang HL. CC chemokine ligand 2 upregulates the current density and expression of TRPV1 channels and Nav1.8 sodium channels in dorsal root ganglion neurons. J Neuroinflammation 2012;9:189.
[35] Kawamata T, Niiyama Y, Yamamoto J, Furuse S. Reduction of bone cancer pain by CB1 activation and TRPV1 inhibition. J Anesth 2010;24: 328–32.
[36] Kawasaki Y, Zhang L, Cheng JK, Ji RR. Cytokine mechanisms of central sensitization: distinct and overlapping role of interleukin-1beta, interleukin-6, and tumor necrosis factor-alpha in regulating synaptic and neuronal activity in the superficial spinal cord. J Neurosci 2008;28: 5189–94.
[37] Kochukov MY, McNearney TA, Yin H, Zhang L, Ma F, Ponomareva L, Abshire S, Westlund KN. Tumor necrosis factor-alpha (TNF-alpha) enhances functional thermal and chemical responses of TRP cation channels in human synoviocytes. Mol Pain 2009;5:49.
[38] Langeslag M, Constantin CE, Andratsch M, Quarta S, Mair N, Kress M. Oncostatin M induces heat hypersensitivity by gp130-dependent sensitization of TRPV1 in sensory neurons. Mol Pain 2011;7:102–7.
[39] Larrucea C, Castro P, Sepulveda FJ, Wandersleben G, Roa J, Aguayo LG. Sustained increase of Ca+2 oscillations after chronic TRPV1 receptor activation with capsaicin in cultured spinal neurons. Brain Res 2008;1218: 70–6.
[40] Lee KM, Jeon SM, Cho HJ. Interleukin-6 induces microglial CX3CR1 expression in the spinal cord after peripheral nerve injury through the activation of p38 MAPK. Eur J Pain 2010;14:682.e1–12.
[41] Lei Q, Malykhina AP. Colonic inflammation up-regulates voltage-gated sodium channels in bladder sensory neurons via activation of peripheral transient potential vanilloid 1 receptors. Neurogastroenterol Motil 2012; 24:575–85, e257.
[42] Li Y, Cai J, Han Y, Xiao X, Meng XL, Su L, Liu FY, Xing GG, Wan Y. Enhanced function of TRPV1 via up-regulation by insulin-like growth factor-1 in a rat model of bone cancer pain. Eur J Pain 2014;18:774–84.
[43] Liang R, Liu X, Wei L, Wang W, Zheng P, Yan X, Zhao Y, Liu L, Cao X. The modulation of the excitability of primary sensory neurons by Ca(2)(+)-CaM-CaMKII pathway. Neurol Sci 2012;33:1083–93.
[44] Liu M, Yang H, Fang D, Yang JJ, Cai J, Wan Y, Chui DH, Han JS, Xing GG. Upregulation of P2X3 receptors by neuronal calcium sensor protein VILIP-1 in dorsal root ganglions contributes to the bone cancer pain in rats. PAIN 2013;154:1551–68.
[45] Liu XD, Yang JJ, Fang D, Cai J, Wan Y, Xing GG. Functional upregulation of nav1.8 sodium channels on the membrane of dorsal root ganglia neurons contributes to the development of cancer-induced bone pain. PLoS One 2014;9:e114623.
[46] Lozano-Ondoua AN, Symons-Liguori AM, Vanderah TW. Cancer-induced bone pain: mechanisms and models. Neurosci Lett 2013;557:52–9.
[47] Manjavachi MN, Motta EM, Marotta DM, Leite DF, Calixto JB. Mechanisms involved in IL-6-induced muscular mechanical hyperalgesia in mice. PAIN 2010;151:345–55.
[48] Mao-Ying QL, Wang XW, Yang CJ, Li X, Mi WL, Wu GC, Wang YQ. Robust spinal neuroinflammation mediates mechanical allodynia in Walker 256 induced bone cancer rats. Mol Brain 2012;5:16–5.
[49] Matsutomi T, Nakamoto C, Zheng T, Kakimura J, Ogata N. Multiple types of Na(+) currents mediate action potential electrogenesis in small neurons of mouse dorsal root ganglia. Pflugers Arch 2006;453:83–96.
[50] Melemedjian OK, Asiedu MN, Tillu DV, Peebles KA, Yan J, Ertz N, Dussor GO, Price TJ. IL-6- and NGF-induced rapid control of protein synthesis and nociceptive plasticity via convergent signaling to the eIF4F complex. J Neurosci 2010;30:15113–23.
[51] Miranda-Morales M, Ochoa-Cortes F, Stern E, Lomax AE, Vanner S. Axon reflexes evoked by transient receptor potential vanilloid 1 activation are mediated by tetrodotoxin-resistant voltage-gated Na+ channels in intestinal afferent nerves. J Pharmacol Exp Ther 2010;334:566–75.
[52] Murakami M, Hibi M, Nakagawa N, Nakagawa T, Yasukawa K, Yamanishi K, Taga T, Kishimoto T. IL-6-induced homodimerization of gp130 and associated activation of a tyrosine kinase. Science 1993;260:1808–10.
[53] Natura G, von Banchet GS, Schaible HG. Calcitonin gene-related peptide enhances TTX-resistant sodium currents in cultured dorsal root ganglion neurons from adult rats. PAIN 2005;116:194–204.

[54] Neelands TR, Jarvis MF, Faltynek CR, Surowy CS. Elevated temperatures alter TRPV1 agonist-evoked excitability of dorsal root ganglion neurons. Inflamm Res 2008;57:404–9.
[55] Nicol GD, Lopshire JC, Pafford CM. Tumor necrosis factor enhances the capsaicin sensitivity of rat sensory neurons. J Neurosci 1997;17:975–82.
[56] Niiyama Y, Kawamata T, Yamamoto J, Furuse S, Namiki A. SB366791, a TRPV1 antagonist, potentiates analgesic effects of systemic morphine in a murine model of bone cancer pain. Br J Anaesth 2009;102:251–8.
[57] Niiyama Y, Kawamata T, Yamamoto J, Omote K, Namiki A. Bone cancer increases transient receptor potential vanilloid subfamily 1 expression within distinct subpopulations of dorsal root ganglion neurons. Neuroscience 2007;148:560–72.
[58] Obreja O, Biasio W, Andratsch M, Lips KS, Rathee PK, Ludwig A, Rose-John S, Kress M. Fast modulation of heat-activated ionic current by proinflammatory interleukin 6 in rat sensory neurons. Brain 2005;128: 1634–41.
[59] Opree A, Kress M. Involvement of the proinflammatory cytokines tumor necrosis factor-alpha, IL-1 beta, and IL-6 but not IL-8 in the development of heat hyperalgesia: effects on heat-evoked calcitonin gene-related peptide release from rat skin. J Neurosci 2000;20:6289–93.
[60] Pan HL, Zhang YQ, Zhao ZQ. Involvement of lysophosphatidic acid in bone cancer pain by potentiation of TRPV1 via PKCepsilon pathway in dorsal root ganglion neurons. Mol Pain 2010;6:85–6.
[61] Peters CM, Ghilardi JR, Keyser CP, Kubota K, Lindsay TH, Luger NM, Mach DB, Schwei MJ, Sevcik MA, Mantyh PW. Tumor-induced injury of primary afferent sensory nerve fibers in bone cancer pain. Exp Neurol 2005;193:85–100.
[62] Planells-Cases R, Valente P, Ferrer-Montiel A, Qin F, Szallasi A. Complex regulation of TRPV1 and related thermo-TRPs: implications for therapeutic intervention. Adv Exp Med Biol 2011;704:491–515.
[63] Qu XX, Cai J, Li MJ, Chi YN, Liao FF, Liu FY, Wan Y, Han JS, Xing GG. Role of the spinal cord NR2B-containing NMDA receptors in the development of neuropathic pain. Exp Neurol 2009;215:298–307.
[64] Rivlin AS, Tator CH. Objective clinical assessment of motor function after experimental spinal cord injury in the rat. J Neurosurg 1977;47:577–81.
[65] Rose-John S, Scheller J, Elson G, Jones SA. Interleukin-6 biology is coordinated by membrane-bound and soluble receptors: role in inflammation and cancer. J Leukoc Biol 2006;80:227–36.
[66] Schaible HG, von Banchet GS, Boettger MK, Brauer R, Gajda M, Richter F, Hensellek S, Brenn D, Natura G. The role of proinflammatory cytokines in the generation and maintenance of joint pain. Ann N Y Acad Sci 2010;1193: 60–9.
[67] Scheller J, Ohnesorge N, Rose-John S. Interleukin-6 trans-signalling in chronic inflammation and cancer. Scand J Immunol 2006;63:321–9.
[68] Smith H, Brooks JR. Capsaicin-based therapies for pain control. Prog Drug Res 2014;68:129–46.
[69] Spooren A, Kolmus K, Laureys G, Clinckers R, De KJ, Haegeman G, Gerlo S. Interleukin-6, a mental cytokine. Brain Res Rev 2011;67:157–83.
[70] Stein AT, Ufret-Vincenty CA, Hua L, Santana LF, Gordon SE. Phosphoinositide 3-kinase binds to TRPV1 and mediates NGF-stimulated TRPV1 trafficking to the plasma membrane. J Gen Physiol 2006;128:509–22.
[71] Tyrrell L, Renganathan M, Dib-Hajj SD, Waxman SG. Glycosylation alters steady-state inactivation of sodium channel Nav1.9/NaN in dorsal root ganglion neurons and is developmentally regulated. J Neurosci 2001;21: 9629–37.
[72] Vallejo R, Tilley DM, Vogel L, Benyamin R. The role of glia and the immune system in the development and maintenance of neuropathic pain. Pain Pract 2010;10:167–84.
[73] Vazquez E, Kahlenbach J, Segond von BG, Konig C, Schaible HG, Ebersberger A. Spinal interleukin-6 is an amplifier of arthritic pain in the rat. Arthritis Rheum 2012;64:2233–42.
[74] von Banchet GS, Kiehl M, Schaible HG. Acute and long-term effects of IL-6 on cultured dorsal root ganglion neurones from adult rat. J Neurochem 2005;94:238–48.
[75] Waxman SG. Channel, neuronal and clinical function in sodium channelopathies: from genotype to phenotype. Nat Neurosci 2007;10:405–9.
[76] Wei XH, Na XD, Liao GJ, Chen QY, Cui Y, Chen FY, Li YY, Zang Y, Liu XG. The up-regulation of IL-6 in DRG and spinal dorsal horn contributes to neuropathic pain following L5 ventral root transection. Exp Neurol 2013; 241:159–68.
[77] Xu Q, Zhang XM, Duan KZ, Gu XY, Han M, Liu BL, Zhao ZQ, Zhang YQ. Peripheral TGF-beta1 signaling is a critical event in bone cancer-induced hyperalgesia in rodents. J Neurosci 2013;33:19099–111.
[78] Yamada O, Ozaki K, Akiyama M, Kawauchi K. JAK-STAT and JAK-PI3K-mTORC1 pathways regulate telomerase transcriptionally and posttranslationally in ATL cells. Mol Cancer Ther 2012;11:1112–21.
[79] Yan J, Melemedjian OK, Price TJ, Dussor G. Sensitization of dural afferents underlies migraine-related behavior following meningeal application of interleukin-6 (IL-6). Mol Pain 2012;8:6–8.
[80] Zhang X, Huang J, McNaughton PA. NGF rapidly increases membrane expression of TRPV1 heat-gated ion channels. EMBO J 2005;24:4211–23.
[81] Zheng Q, Fang D, Cai J, Wan Y, Han JS, Xing GG. Enhanced excitability of small dorsal root ganglion neurons in rats with bone cancer pain. Mol Pain 2012;8:24–8.
[82] Zheng Q, Fang D, Liu M, Cai J, Wan Y, Han JS, Xing GG. Suppression of KCNQ/M (Kv7) potassium channels in dorsal root ganglion neurons contributes to the development of bone cancer pain in a rat model. PAIN 2013;154:434–48.
[83] Zhuang ZY, Xu H, Clapham DE, Ji RR. Phosphatidylinositol 3-kinase activates ERK in primary sensory neurons and mediates inflammatory heat hyperalgesia through TRPV1 sensitization. J Neurosci 2004;24:8300–9.
[84] Zimmermann M. Ethical guidelines for investigations of experimental pain in conscious animals. PAIN 1983;16:109–10.
[85] Zimmermann M. Pathobiology of neuropathic pain. Eur J Pharmacol 2001;429:23–37.